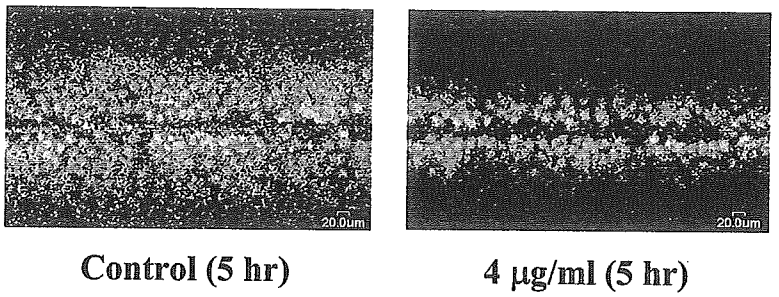

Fig. 3. Inhibition of GJIC in WB cells after MX treatment.

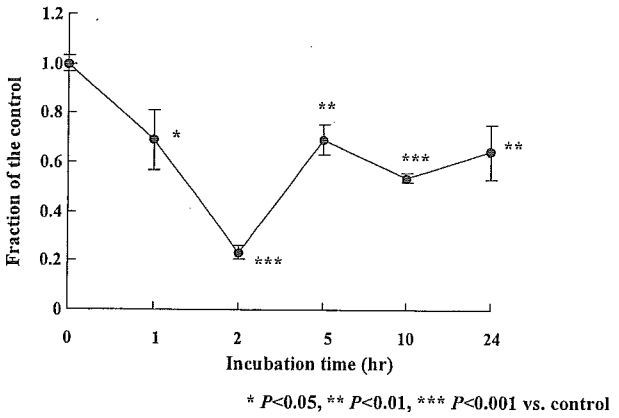

Fig. 4. Time course of GJIC in WB cells after MX treatment. Values are means ± SD of data from assays performed in triplicate.

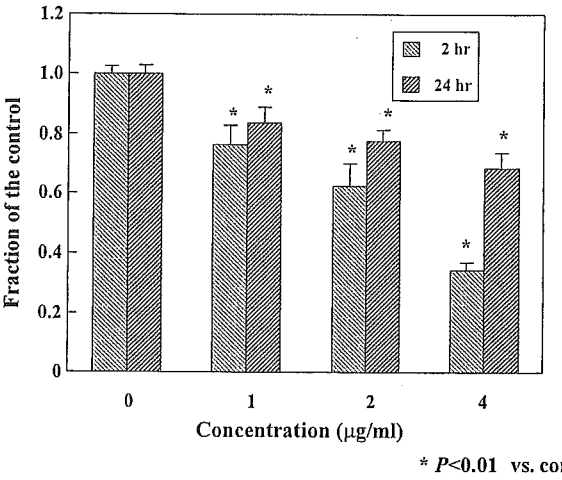

Fig. 5. Dose-dependent inhibition of GJIC in WB cells after MX treatment. Values are means ± SD of data from assays performed in triplicate.

moters including non-liver tumor promoters like TPA, have the ability to inhibit cell–cell communication in WB cells [Loewenstein, 1979; Trosko et al., 1983; Trosko and Goodman, 1994; Evans and Martin, 2002].

It has been suggested that MX might primarily affect the mucosa of the alimentary tract, when exposure levels are sufficient to overwhelm the defense capacity relying on glutathione or other factors, or when defense systems are impaired [Nishikawa et al., 1994; Meier et al., 1996]. Previously, we reported that MX induces cell proliferation in the gastric mucosa of rats even at low, nontoxic doses such as 25 ppm [Nishikawa et al., 1994] as well as at higher doses [Furihata et al., 1992]. In this context, mitogenic potential, in addition to possible regenerative responses, have been suggested to be involved in the mechanisms underlying stomach tumor-promoting activity [Nishikawa et al., 1999]. Nevertheless, in the present study, cell proliferation was not increased by the MX treatments in any of the organs examined, including the gastrointestinal tract, suggesting the possible existence of species differences. It is conceivable that tumor-promoting processes are species-specific in some cases, but except for limited in vivo mutagenicity assays [Yoshikawa et al., 1982; Nohmi et al., 1983; Madle et al., 1986 Degawa et al., 1990], there is little evidence that tumor-initiating processes might similarly differ with the animal species.

In conclusion, the results of the present study indicate that MX inhibits GJIC in cultured rat WB cells but is not mitogenic, mutagenic, or carcinogenic in *gpt* delta mice. Thus the carcinogenicity of MX in rats may be, at least partially, associated with tumor-promoting effects. It remains to be determined whether MX is mutagenic in transgenic rats, such as the Big Blue or *gpt* delta rat.

ACKNOWLEDGMENTS

This study was supported by Grants-in-Aid for Health Sciences from the Ministry of Health, Labour and Welfare, Japan.

REFERENCES

Borenfeund E, Puerna JA. 1985. Toxicity determined in vitro by morphological alteration and neutral red absorption. Toxicol Lett 24: 119–124.

Daniel FB, Olson GR, Stober JA. 1991. Induction of gastrointestinal tract nuclear anomalies in B6C3F1 mice by 3-chloro-4-(dichloromethyl)-5-hydroxy-2(5*H*)-furanone and 3,4-(dichloro)-5-hydroxy-2[5*H*]-furanone mutagenic byproducts of chlorine disinfection. Environ Mol Mutagen 17:32–39.

Degawa M, Agatsuma T, Hashimoto Y. 1990. Species difference among experimental rodents in the activity and induction of cytochrome

P-450 isozymes for mutagenic activation of carcinogenic aromatic amines. Jpn J Cancer Res 81:1253–1258.

El-Fouly MH, Trosko JE, Chang CC. 1987. Scrape loading and dye transfer: a rapid and simple technique to study gap junctional intercellular communication. Exp Cell Res 168:422–430.

Evans WH, Martin PEM. 2002. Gap junctions: structure and function. Mol Membr Biol 19:121–136.

Franzen R, Tanabe K, Morita M. 1998. Isolation of a MX-guanine adduct formed at physiological conditions. Chemosphere 36: 2803–2808.

Furihata C, Yamashita M, Kinae N, Matsushima T. 1992. Genotoxicity and cell proliferative activity of 3-chloro-4-(dichloromethyl)-5-hydroxy-2(5*H*)-furanone [MX] in rat glandular stomach. Wat Sci Tech 25:341–345.

Geter DR, Winn RN, Fournie JW, Norris MB, DeAngelo AB, Hawkins WE. 2004. MX [3-chloro-4-(dichloromethyl)-5-hydroxy-2[5*H*]-furanone], a drinking-water carcinogen, does not induce mutations in the liver of *cII* transgenic medaka (*Oryzias latipes*). J Toxicol Environ Health A 67:373–83.

Gorelick NJ, Mirsalis JC. 1996. A strategy for the application of transgenic rodent mutagenesis assays. Environ Mol Mutagen 28:434–442.

Grassilli E, Carcereri de Prati A, Monti D, Troiano L, Menegazzi M, Barbieri D, Franceschi C, Suzuki H. 1992. Studies of the relationship between cell proliferation and cell death: II. Early gene expression during concanavalin A-induced proliferation or dexamethasone-induced apoptosis of rat thymocytes. Biochem Biophys Res Commun 188:1261–1266.

Hemming J, Holmbolm B, Reunanen M, Kronberg L. 1986. Determination of the strong mutagen 3-chloro-4-(dichloromethyl)-5-hydroxy-2(5*H*)-furanone in chlorinated drinking and humic water. Chemosphere 15:549–556.

Horiguchi M, Masumura K, Ikehata H, Ono T, Kanke Y, Nohmi T. 2001. Molecular nature of UVB-induced deletions in the murine epidermis. Cancer Res 61:3913–3918.

Horth H, Fielding M, Gibson T, James HA, Ross H. 1989. Identification of mutagens in drinking water. Water Research Centre Technical Report PRD 2038-M, Medmenham, England.

Huuskonen H, Venalainen R, Komulainen H. 2003. Developmental toxicity evaluation of 3-chloro-4-(dichloromethyl)-5-hydroxy-2(5*H*)-furanone (MX) in Wistar rats. Birth Defects Res B 68:172–179.

Ishiguro Y, Santodonato J, Neal MW. 1988. Mutagenic potency of chlorofuranones and related compounds in Salmonella. Environ Mol Mutagen 11:225–234.

Kinae N, Sugiyama C, Nasuda MY, Goto K, Tokumoto K, Furugori M, Shimoi K. 1992. Seasonal variation and stability of chlorinated organic mutagens in drinking water. Wat Sci Tech 25:333–340.

Komulainen H, Kosma V-M, Vaittinen S-L, Vartiainen T, Kaliste-Korhonen E, Lötjönen S, Tuominen RK, Tuomisto J. 1997. Carcinogenicity of the drinking water mutagen 3-chloro-4-(dichloromethyl)-5-hydroxy-2(5*H*)-furanone in the rat. J Natl Cancer Inst 89:848–856.

Kronberg L, Vertiainen T. 1988. Ames mutagenicity and concentration of the strong mutagen 3-chloro-4-(dichloromethyl)-5-hydroxy-2(5*H*)-furanone and its geometric isomer E-2-chloro-3-(dichloromethyl)-4-oxo-butenoic acid in chlorine-treated tap water. Mutat Res 206:177–182.

LaLonde RT, Cook GP, Perakyla H, Dence CW, Babish JG. 1991. *Salmonella typhimurium* (TA100) mutagenicity of 3-chloro-4-(dichloromethyl)-5-hydroxy-2(5*H*)-furanone and its open- and closed-ring analogs. Environ Mol Mutagen 17:40–48.

LaLonde RT, Xie S. 1993. Glutathione and *N*-acetylcysteine inactivation of mutagenic 2(5H)-furanones from the chlorination of humics in water. Chem Res Toxicol 6:445–451.

Loewenstein WR. 1979. Junctional intercellular communication and the control of growth. Biochim Biophys Acta 560:1–65.

Madle E, Korte A, Beek B. 1986. Species differences in mutagenicity testing: I. Micronucleus and SCE tests in rats, mice, and Chinese hamsters with aflatoxin B_1. Teratog Carcinog Mutagen 6:1–13.

Masumura K, Kuniya K, Kurobe T, Fukuoka M, Yatagai F, Nohmi T. 2002. Heavy-ion-induced mutations in the *gpt* delta transgenic mouse: Comparison of mutation spectra induced by heavy-ion, X-ray and γ-ray radiation. Environ Mol Mutagen 40:207–215.

Matsumura H, Watanabe M, Matsumoto K, Ohta T. 1994. 3-Chloro-4-(dichloromethyl)-5-hydroxy-2(5*H*)-furanone (MX) induces gene mutations and inhibits metabolic cooperation in cultured Chinese hamster cells. J Toxicol Environ Health 43:65–72.

Meier JR, Knohl RB, Coleman WE, Ringhand HP, Munch JW, Kaylor WH, Streicher RP, Kopfler FC. 1987a. Studies on the potent bacterial mutagen, 3-chloro-4-(dichloromethyl)-5-hydroxy-2(5*H*)-furanone: aqueous stability, XAD recovery and analytical determination in drinking water and in chlorinated humic acid solution. Mutat Res 189:363–373.

Meier JR, Blazak WF, Knohl RB. 1987b. Mutagenic and clastogenic properties of 3-chloro-4-(dichloromethyl)-5-hydroxy-2(5*H*)-furanone: a potent bacterial mutagen in drinking water. Environ Mol Mutagen 10:411–424.

Meier JR, Monarca S, Patterson KS, Villarini M, Daniel FB, Moretti M, Pasquini R. 1996. Urine mutagenicity and biochemical effects of the drinking water mutagen, 3-chloro-4-(dichloromethyl)-5-hydroxy-2(5*H*)-furanone (MX), following repeated oral administration to mice and rats. Toxicology 110:59–70.

Melnick RL, Boorman GA, Dellarco V. 1997. Water chlorination, 3-chloro-4-(dichloromethyl)-5-hydroxy-2(5*H*)-furanone (MX), and potential cancer risk. J Natl Cancer Res 89:832–833.

Muir WM, Howard RD. 1999. Possible ecological risks of transgenic organism release when transgenes affect mating success: sexual selection and the Trojan gene hypothesis. Proc Natl Acad Sci USA 96:13853–13856.

Munter T, Le Curieux F, Sjoholm R, Kronberg L. 1998. Reaction of the potent bacterial mutagen 3-chloro-4-(dichloromethyl)-5-hydroxy-2(5*H*)-furanone (MX) with 2′-deoxyadenosine and calf thymus DNA: identification of fluorescent propenoformyl derivatives. Chem Res Toxicol 11:226–233.

Nishikawa A, Kinae N, Furukawa F, Mitsui M, Enami T, Hasegawa T, Takahashi M. 1994. Enhancing effects of 3-chloro-4-(dichloromethyl)-5-hydroxy-2(5*H*)-furanone on cell proliferation and lipid peroxidation in the rat gastric mucosa. Cancer Lett 85:151–157.

Nishikawa A, Furukawa F, Lee I-S, Kasahara K, Tanakamaru Z, Nakamura H, Miyauchi M, Kinae N, Hirose M. 1999. Promoting effects of 3-chloro-4-(dichloromethyl)-5-hydroxy-2(5*H*)-furanone on rat glandular stomach carcinogenesis initiated with *N*-methyl-*N*′-nitro-*N*-nitrosoguanidine. Cancer Res 59:2045–2049.

Nohmi T, Yoshikawa K, Nakadate M, Ishidate M Jr. 1983. Species difference in the metabolic activation of phenacetin by rat and hamster liver microsomes. Biochem Biophys Res Commun 110:746–752.

Nohmi T, Katoh M, Suzuki M, Matsui M, Yamada M, Watanabe M, Suzuki H, Horiya N, Ueda O, Shibuya T, Ikeda H, Sofuni T. 1996. A new transgenic mouse mutagenesis test system using Spi$^-$ and 6-thioguanine selections. Environ Mol Mutagen 28:465–470.

Nohmi T, Suzuki M, Masumura K, Yamada M, Matsui K, Ueda O, Suzuki H, Katoh M, Ikeda H, Sofuni T. 1999. Spi$^-$ selection: an efficient method to detect γ-ray-induced deletions in transgenic mice. Environ Mol Mutagen 34:9–15.

Nohmi T, Suzuki T, Masumura K. 2000. Recent advances in the protocols of transgenic mouse mutation assays. Mutat Res 455:191–215.

Padmapria AA, Just G, Lewis NG. 1985. Synthesis of 3-chloro-4-(dichloromethyl)-5-hydroxy-2(5*H*)-furanone, a potent mutagen. Can J Chem 63:828–832.

Sai K, Upham BL, Kang K-S, Hasegawa R, Inoue T, Trosko JE. 1998. Inhibitory effect of pentachlorophenol on gap junctional intercellular communication in rat liver epithelial cells in vitro. Cancer Lett 130:9–17.

Suzuki N, Nakanishi J. 1990. The determination of strong mutagen, 3-chloro-4-(dichloromethyl)-5-hydroxy-2(5*H*)-furanone in Japan. Chemosphere 21:387–392.

Takeiri A, Mishima M, Tanaka K, Shioda A, Ueda O, Suzuki H, Inoue M, Masumura K, Nohmi T. 2003. Molecular characterization of mitomycin C-induced large deletions and tandem-base substitutions in the bone marrow of *gpt* delta transgenic mice. Chem Res Toxicol 16:171–179.

Thilly WG. 2003. Have environmental mutagens caused oncomutations in people? Nat Genet 34:255–259.

Trosko JE. 1997. Challenge to the simple paradigm that 'carcinogens' are 'mutagens' and to the in vitro and in vivo assays used to test the paradigm. Mutat Res 373:245–249.

Trosko JE, Chang CC. 1988. Nongenotoxic mechanisms in carcinogenesis: Role of inhibited intercellular communication. In: Carcinogen Risk Assessment: New Directions in the Qualitative and Quantitative Aspects. NY:Cold Spring Harbor. Cold Spring Harbor Laboratory Banbury Report 31. pp 139–170.

Trosko JE, Goodman JI. 1994. Intercellular communication may facilitate apoptosis: implications for tumor promotion. Mol Carcinog 11:8–12.

Trosko JE, Ruch RJ. 1998. Cell-cell communication in carcinogenesis. Front Biosci 3:208–236.

Trosko JE, Ruch RJ. 2003. Gap junctions as targets for cancer chemoprevention and chemotherapy. Curr Drug Targets 3:465–482.

Trosko JE, Chang CC, Medcalf A. 1983. Mechanisms of tumor promotion: potential role of intercellular communication. Cancer Invest 1:511–526.

Tsao MS, Smith JD, Nelson KG, Grisham JW. 1984. A diploid epithelial cell line from normal adult rat liver with phenotypic properties of 'oval' cells. Exp Cell Res 154:38–52.

Watanabe M, Kobayashi H, Ohta T. 1994. Rapid inactivation of 3-chloro-4-(dichloromethyl)-5-hydroxy-2(5*H*)-furanone (MX), a potent mutagen in chlorinated drinking water, by sulfhydryl compounds. Mutat Res 312:131–138.

Wilson MR, Close TW, Trosko JE. 2000. Cell population dynamics (apoptosis, mitosis, and cell-cell communication) during disruption of homeostasis. Exp Cell Res 254:257–268.

Yoshikawa K, Nohmi T, Miyata R, Ishidate M Jr., Ozawa N, Isobe M, Watabe T, Kada T, Kawachi T. 1982. Difference in liver homogenates from Donryu, Fischer, Sprague-Dawley and Wistar strains of rat in the drug-metabolizing enzyme assay and the *Salmonella*/hepatic S9 activation test. Mutat Res 96:167–186.

Yotti LP, Chang CC, Trosko JE. 1979. Elimination of metabolic cooperation in Chinese hamster cells by a tumor promoter. Science 206:1089–1091.

Carcinogenesis vol.26 no.11 pp.1947–1955, 2005
doi:10.1093/carcin/bgi156
Advance Access publication June 16, 2005

Mechanisms of chemopreventive effects of 8-methoxypsoralen against 4-(methylnitrosamino)-1-(3-pyridyl)-1-butanone-induced mouse lung adenomas

Masafumi Miyazaki, Hiroshi Yamazaki, Hijiri Takeuchi[1], Kousuke Saoo[1], Masanao Yokohira[1], Ken-ichi Masumura[2], Takehiko Nohmi[2], Yoshihiko Funae[3], Katsumi Imaida[1] and Tetsuya Kamataki*

Graduate School of Pharmaceutical Sciences, Hokkaido University, Sapporo 060-0812, Japan, [1]Faculty of Medicine, Kagawa University, Kagawa 761-0793, Japan, [2]National Institute of Health Sciences, Tokyo 158-8501, Japan and [3]Osaka City University Medical School, Osaka 545-8585, Japan

*To whom correspondence and reprint requests should be addressed at: Laboratory of Drug Metabolism, Graduate School of Pharmaceutical Sciences, Hokkaido University, N12W6, Kita-ku, Sapporo 060-0812, Japan. Tel: +81 11 706 3233; Fax: +81 11 706 4978; E-mail: SNC78123@nifty.com

Recently we reported that the occurrence of lung adenoma caused by 4-(methylnitrosamino)-1-(3-pyridyl)-1-butanone (NNK) was completely prevented by pretreatment of female A/J mice with 8-methoxypsoralen, a potent inhibitor of cytochrome P450 (P450 or CYP) 2A [Takeuchi *et al.* (2003) *Cancer Res.*, 63, 7581–7583]. Thus, the aim of this study was to confirm that 8-methoxypsoralen exhibits chemopreventive effects by inhibiting CYP2A in the mouse lung. The involvement of CYP2A in the metabolic activation of NNK in the lung was first evidenced by the fact that the mutagenic activation of NNK by mouse lung microsomes was inhibited by 8-methoxypsoralen, coumarin and antibodies to rat CYP2A1. Supporting this, the mutagenic activation of NNK was efficiently catalyzed by mouse CYP2A4 and CYP2A5 co-expressed with NADPH-P450 reductase in a genetically engineered *Salmonella typhimurium* YG7108. The expression of mRNA for CYP2A5, but not for CYP2A4 or CYP2A12, in the mouse lung was proven by reverse transcriptase–polymerase chain reaction, probably indicating that CYP2A5 present in the mouse lung was involved in the metabolic activation of NNK. In accordance with these *in vitro* data, treatment of *gpt delta* transgenic mice with 8-methoxypsoralen prior to NNK completely inhibited the mutation of the *gpt delta* gene. The *in vivo* chemopreventive effects of 8-methoxypsoralen towards NNK-induced adenoma was seen only when the agent was given to female A/J mice prior to, but not posterior to, NNK, lending support to the idea that NNK is activated by CYP2A5 in the mouse lung as an initial step to cause adenoma. The inhibition by 8-methoxypsoralen of NNK-induced adenoma was seen in a dose-dependent manner: the dose to show apparent 50% suppression was calculated to be 1.0 mg/kg. To our surprise, CYP2A protein(s) was expressed in the lesion of NNK-induced lung adenomas, probably suggesting that 8-methoxypsoralen could inhibit the possible occurrence of further mutation of the adenoma cells induced by NNK. Based on these lines of evidence, we propose that 8-methoxypsoralen inhibits the CYP2A5-mediated metabolic activation of NNK in the mouse lung, leading to the prevention of NNK-induced adenoma.

Introduction

Tobacco smoke contains >4000 components; at least 60 chemicals including nitrosamines are proven to be carcinogenic. Among them, NNK, a tobacco-specific *N*-nitrosamine, is believed to be one of the most promising candidates of lung carcinogen in humans, since NNK is known to induce lung tumors in laboratory animals such as mice, rats and hamsters (1–4). NNK is known to be metabolically activated to elicit their genotoxicity (1,5). The first activation step of NNK is thought to be the methylene or methyl hydroxylation of the carbon atom located at the α-position of the *N*-nitroso group primary mediated by P450, leading to the formation of electrophiles which can methylate or pyridyloxobutylate DNA, respectively (1). This initial event has been reported to result in the formation of O^6-methylguanine, an adduct that leads to GC→AT transitional mispairing and the subsequent activation of the K-*ras* proto-oncogene (6,7), an initiating event in tumor development.

P450 is a heme-containing enzyme responsible for the oxidation of a wide variety of exogenous compounds such as drugs, environmental pollutants and foodstuffs, and endogenous compounds including steroids, fatty acids and prostaglandins (8–10). Some of the oxidative reactions catalyzed by P450 result in the formation of reactive intermediates, which bind to endogenous macromolecules such as DNA, RNA and proteins to induce organ toxicities (11,12). Thus, the catalytic property and the content of P450 can be considered to be the determinants of the formation of reactive metabolites and the subsequent toxicity of chemicals.

CYP2A6 is one of the major members of P450 expressed in human livers (13) and to lesser amounts in the lung (14,15). This cytochrome is involved in the mutagenic activation of a wide variety of promutagens including NNK (5,16,17). The genetic polymorphism of *CYP2A6* was originally discovered as one of the causes of inter-individual differences in the metabolism of coumarin (18,19). In further study by us, we first found the novel deletion-type mutants of the *CYP2A6* gene (*CYP2A6*4A* and **4B*). Following this, we also found single nucleotide polymorphisms (CYP2A6**7* and **11*), reducing CYP2A6 enzymatic activities in a Japanese population (20–23). Combining these two concepts that CYP2A6 is capable of activating NNK and that there are genetic polymorphisms in *CYP2A6*, we hypothesized that subjects harboring these

Abbreviations: ABC, avidin-biotin complex; CPR, NADPH-cytochrome P450 reductase (EC 1.6.2.4, NADPH:ferrihemoprotein reductase); CYP, individual forms of cytochrome P450 (EC 1.14.14.1); ENU, ethylnitrosourea; NNK, 4-(methylnitrosamino)-1-(3-pyridyl)-1-butanone; P450, general term for cytochrome P450; PCR, polymerase chain reaction; RT, reverse transcriptase.

Carcinogenesis vol.26 no.11 © Oxford University Press 2005; all rights reserved.

lleles of the *CYP2A6* gene have less risk for tobacco-related ıng cancer. Our large-scale epidemiological studies clearly ıpported this idea (24–26). Based on these results, it was ssumed that CYP2A6 determines the cancer risk caused by ɔbacco-smoking via its ability to activate the nitrosamines. lowever, it was necessary to further ascertain this idea using xperimental animals.

8-Methoxypsoralen is a naturally occurring furanocoumarin erivative found in many plant species such as celery, figs, mes, parsnip and parsley (27). Oral administration of -methoxypsoralen, followed by ultraviolet A light, has pho-ɔsensitizing effects. Thus, this drug has been used clinically ɔr the treatments of psoriasis (28,29). 8-Methoxypsoralen is lso known as a potent mechanism-based inhibitor of CYP2A6 nd the orthologous forms, mouse CYP2A5 and rat CYP2A3 30–32). Recently, we demonstrated that lung tumorigenesis aused by NNK was completely suppressed in female A/J mice vhich had been pretreated with 8-methoxypsoralen (33), prob-bly indicating that 8-methoxypsoralen prevented the occur-ence of the lung tumorigenesis by inhibiting the metabolic ctivation of NNK catalyzed by CYP2As present in the lungs ıf mice. However, we still needed to provide direct evidence .s to whether or not 8-methoxpsoralen inhibited the mutagenic .ctivation of NNK.

Thus, in the present study, we first examined the inhibitory ffects of 8-methoxypsoralen on the mutagenic activation of NNK by both liver or lung microsomes from mice and the orms of mouse CYP2A (CYP2A4, CYP2A5 or CYP2A12) xpressed in the *Salmonella typhimurium* YG7108. To evalu-ıte the *in vivo* effects of 8-methoxypsoralen on the muta-ɡenicity and tumorigenicity of NNK *in vivo*, we carried out wo assays using the *gpt delta* transgenic mice carrying a ıhuttle vector as a monitor of mutation and using female A/J nice as an experimental animal model for lung tumorigenesis, espectively. Based on results presented in this paper, we pro-ɔose that suppression of the initiation step of carcinogenesis ɔy pretreatment with CYP2A inhibitors can result in the ɔhemoprevention of lung cancer caused by tobacco smoking.

Materials and methods

Animals and chemicals

Seven-week-old female C57BL/6J mice, 9-week-old female C57BL/6J transgenic mice homozygous for the *gpt delta* gene and 5-week-old female A/J mice (Japan SLC, Shizuoka, Japan) were used. NNK (purity >99%) was purchased from Toronto Research Chemicals (Toronto, Canada). ENU and 8-methoxypsoralen were obtained from Sigma (St Louis, MO). All other chemicals and solvents were of the highest grade commercially available.

Expression of CYP2A in S.typhimurium YG7108 cells

Original *S.typhimurium* YG7108 and three strains of the genetically engineered *S.typhimurium* YG7108 cells, each co-expressing a mouse CYP2A and CPR established previously in our laboratory, were used. The P450 and CPR in the genetically engineered *S.typhimurium* YG7108 cells were expressed according to the method previously described by Fujita *et al.* (34). The content of P450 holo-protein in the *S.typhimurium* cells was determined by Fe^{2+}·CO versus Fe^{2+} difference spectra according to the method of Omura and Sato (35). The expression levels of P450 ranged from 77 nmol/l culture for CYP2A4 to 340 nmol/l culture for CYP2A12. The activity of CPR in sonicated bacterial cells was measured with cytochrome *c* as an electron acceptor by measuring the absorbance change at 550 nm at 20°C according to the method of Philips and Langdon (36). The unit of CPR was defined as the amount of the enzyme that reduced 1 μmol of cytochrome *c*/min. The molar ratio of the expressed CPR to P450 varied from 1.0 for CYP2A12 to 1.9 for CYP2A4.

Mutation assays

The mutation assay with the parental YG7108 cells was performed as described by Maron and Ames (37), with modifications. Briefly, when needed, NNK was metabolically activated outside the *S.typhimurium* YG7108 cells. The effects of the specific inhibitor of P450 forms on the activation of NNK by liver or lung microsomes from mice were examined. The liver and lung microsomes (70 pmol of total P450/reaction) from 7-week-old female C57BL/6J mice were added, which had been suspended in 10 mM Tris–HCl buffer (pH 7.4) containing 1.0 mM ethylenediaminetetraaceticacid and 20% (v/v) glycerol as described previously (38). The parental *S.typhimurium* YG7108 cells were pre-exposed to 100 or 1000 μM of NNK in the presence or absence of various concentrations of specific inhibitors, substrates or antibodies of P450 at 37°C for 20 min before plating. The modifiers employed were α-naphthoflavone (CYP1A), coumarin (CYP2A), 8-methoxypsoralen (CYP2A), chloramphenicol (CYP2B), tolbutamide (CYP2C), quinidine (CYP2D), chlorzoxazone (CYP2E1) and ketoconazole (CYP3A). All inhibitors were dissolved in dimethylsulfoxide to give a final concentration of the organic solvent in the incubation mixtures lower than 1%. Antibodies against rat CYP2A1 raised in rabbits were added to the reaction mixtures (up to 50 μl/mg protein). The mixtures were preincubated at 25°C for 30 min, followed by the addition of NNK as previously described. An NADPH-generating system was added to the reaction mixtures to start incubations.

When the genetically engineered *S.typhimurium* YG7108 was used, NNK was metabolically activated inside the bacterial cells without addition of any other enzymes. In this experiment, the mutagen-producing activity of a form of mouse CYP2As in the activation of NNK was expected to be clarified. The *Salmonella* cells were first pre-exposed to 0.1–250 nM of NNK for 20 min before plating. The NADPH-generating system was not added to the reaction mixtures since the mutagenic activation of promutagens was not affected by the addition of NADPH, probably because NADPH present in the bacterial cells was utilized as an electron donor. The plates were incubated at 37°C for 2 days. Assays were carried out at least twice in duplicate. When the variability of the values of duplicate determinations was within ±20%, the results were adopted. Induced revertants/pmol P450 were calculated based on the increased colonies per pmol of P450 content expressed in the tester strain. The spontaneous revertant number per plate ranged from 20 to 40. Apparent kinetic analysis for the activation of NNK was performed using a computer program (Microcal Origin, Microcal Software, Northampton, MA) designed for non-linear regression analysis. The concentration of 8-methoxypsoralen which decreased the number of revertants to 50% of control (in the absence of 8-methoxypsoralen) was defined as IC_{50}.

Detection of CYP2As in the mouse lung

Total RNAs were prepared from the lung or liver of the 9-week-old female C57BL/6J mouse using RNeasy® Midi kit (QIAGEN, Hilden, Germany). To examine the expression levels of CYP2A mRNA in the mouse tissues, reverse transcriptase–polymerase chain reaction (RT–PCR) was carried out. Total RNA (1 μg) and oligodeoxythymidylic acid primer (0.5 μg) were mixed, incubated at 70°C for 10 min and then cooled on ice. Subsequently, moloney murine leukemia virus reverse transcriptase (20 units) (Toyobo, Tokyo, Japan), RNase inhibitor (20 U) (Takara, Tokyo, Japan), and 0.5 mM, each of four deoxynucleoside triphosphates, were added to the RNA-primer mixtures and then incubated at 42°C for 50 min. PCR was performed in a solution containing cDNA synthesized in the above reaction mixtures (1 μM), 1.5 mM $MgCl_2$, 0.2 mM each of four deoxynucleoside triphosphates, each primer (1 μM), AmpliTaq Gold polymerase (2.5 U) (PerkinElmer Life Sciences) and 10× AmpliTaq reaction buffer (5 μl) (PerkinElmer Life Sciences). PCR was carried out under the following conditions: 30 cycles of reactions composed of cycle denaturation at 94°C for 1 min, annealing at 55°C for 1 min and extension at 72°C for 2 min. The PCR products (96 bp for CYP2A4 and CYP2A5 and 143 bp for CYP2A12) were subjected to a 2% agarose gel and then visualized by ethidium bromide staining. The sequences of primers used are as follows: CYP2A4, 5′-GCCAGCTCTATGAGATGTTT-3′ and 5′-TTATAAAGTC-CTCCAGGCCT-3′; CYP2A5, 5′-GCCAGGTCTATGAGATGTTT-3′ and 5′-TTATAAAGTCCTCCAGGCCC-3′; CYP2A12, 5′-TTAGCTCCATTGT-CTTCGGC-3′ and 5′-GGTACTTCATAACTGAATGG-3′; β-actin, 5′-ATTG-CTGACAGGATGCAGA-3′ and 5′-GCTCAGGAGGAGCAATGATCTT-3′.

gpt mutation assay

The *gpt delta* C57BL/6J transgenic mice were maintained in the Animal Facility of the Faculty of Pharmaceutical Sciences, Hokkaido University, according to the institutional animal care guidelines. The animals were housed in polycarbonate cages with white wood chips for bedding and given free access to drinking water and a basal diet, Oriental MF (Oriental Yeast, Tokyo, Japan), under controlled conditions of humidity (55 ± 5%), lighting (12 h light/dark cycle) and temperature (23 ± 1°C). The animals were pretreated with 8-methoxypsoralen at a dose of 12.5 or 50 mg/kg body wt in 0.2 ml of corn oil or an equal volume of corn oil as a vehicle control via stomach tube daily for 7 days. One hour after the third treatment, the animals were treated with a single i.p. injection of NNK or ENU at a dose of 100 mg/kg body wt or an equal

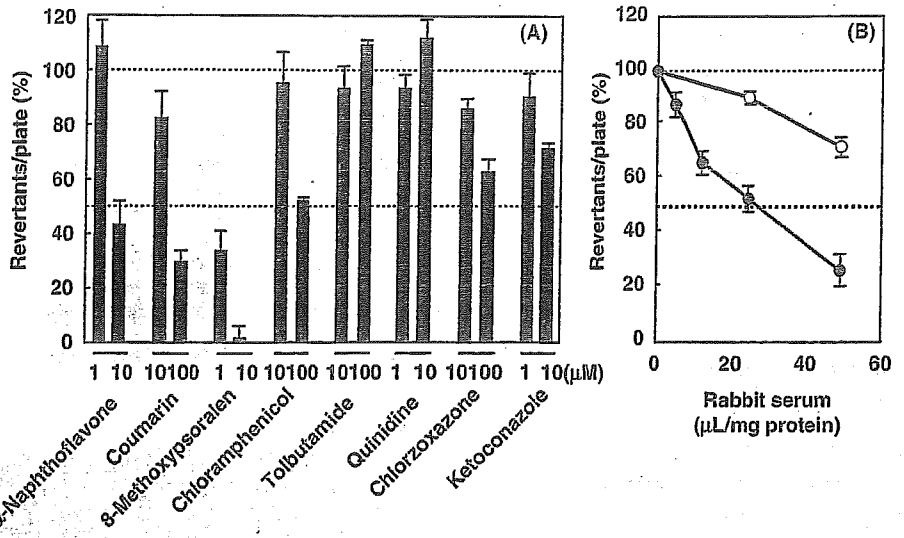

Fig. 1. Effects of specific inhibitors of forms of P450 (A) and anti-CYP2A1 antibodies (B) on the mutagenic activation of NNK catalyzed by mouse liver microsomes. The number of NNK-induced revertants without the inhibitors (A) or sera (B) was 103 revertants/plate. (A) The inhibitors employed were α-naphthoflavone (for CYP1A), coumarin (CYP2A), 8-methoxypsoralen (CYP2A), chloramphenicol (CYP2B), tolbutamide (CYP2C), quinidine (CYP2D), chlorzoxazone (CYP2E1) and ketoconazole (CYP3A). (B) Open and closed circles represent the results with rabbit antiserum to rat CYP2A1 and preimmune serum, respectively. Each value and bar indicates the mean and SD (range) of duplicate determinations, respectively.

volume of saline as a vehicle control. Two weeks after the final treatment, mice were killed under ether anesthesia. They were quickly frozen in liquid nitrogen and stored at −80% until analysis. The *gpt* mutagenesis assay was performed as previously described (39).

Tumorigenicity test

Female A/J mice were maintained in the Animal Facility of the Faculty of Medicine, Kagawa University, according to the institutional animal care guidelines. The animals were housed in polycarbonate cages with white wood chips for bedding and given free access to drinking water and a basal diet, Oriental MF (Oriental Yeast), under controlled conditions of humidity at 60 ± 10%, lighting with 12 h light/dark cycle and temperature at 24 ± 2°C.

The animals were pretreated with 8-methoxypsoralen at a dose of 0.125, 1.25 or 12.5 mg/kg body wt in 0.2 ml corn oil or an equal volume of corn oil as a vehicle control via stomach tube, daily for 3 days. One hour after the last pretreatment, animals were given a single dose of NNK at a dose of 100 mg/kg body wt in 0.1 ml saline via p.o. or an equal volume of saline as a vehicle control. The experiment was terminated at 16 weeks after the first 8-methoxypsoralen pretreatment. In separate experiments, three daily doses of 8-methoxypsoralen (12.5 mg/kg) were given to mice 1, 3 and 7 days after a single dose of NNK injection. At autopsy, their lungs were excised and weighed, infused with 10% neutral buffered formalin and carefully inspected grossly. All of the macroscopically detected lung nodules were counted, and each lung lobe was examined histopathologically. Lung lesions, hyperplasias and adenomas were diagnosed according to the criteria of 'Tumors of the Mouse' (40), and the number of hyperplasias and adenomas was counted under a microscope.

Immunohistochemistry

Lungs were immunostained for CYP2A by the ABC method, all staining processes from deparaffinization to counterstaining with hematoxylin being performed automatically using the Ventana Discovery™ staining system (Ventana Medical Systems, AZ, USA). Anti rabbit CYP2A1 polyclonal antibodies were used at 1:50 dilution.

Statistical analysis

The incidence of lung proliferative lesions were analyzed by the Fisher's exact probability test and data for multiplicity by Student's *t*-test.

Results

Effects of CYP2A inhibitors and anti-CYP2A antibodies on the mutagenic activation of NNK catalyzed by liver and lung microsomes from mice

To estimate a possible P450 form(s) responsible for the mutagenic activation of NNK in mice, effects of the representative inhibitors of P450s and anti-P450 antibodies on the genotoxic activation of NNK catalyzed by liver and lung microsomes from mice were examined. Among the inhibitors tested, coumarin and 8-methoxypsoralen, the inhibitor of CYP2A, efficiently inhibited the mutagenic activation of NNK catalyzed by liver microsomes (Figure 1A). Anti-CYP2A1 antibodies efficiently inhibited the activation of NNK by mouse liver microsomes (Figure 1B).

As was seen with liver microsomes, 8-methoxypsoralen and anti-CYP2A1 antibodies inhibited the mutagenic activation of NNK catalyzed by lung microsomes in a dose-dependent manner (Figure 2).

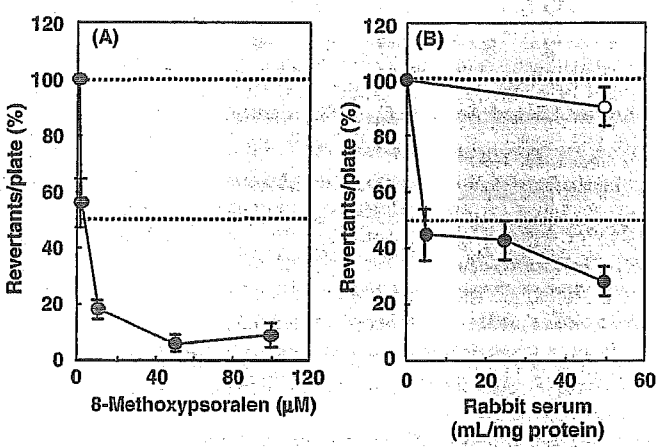

Fig. 2. Inhibition by 8-methoxypsoralen (A) and antiserum to rat CYP2A1 (B) of the mutagenic activation of NNK catalyzed by mouse lung microsomes. The number of NNK-induced revertants without 8-methoxypsoralen (A) and sera (B) was 85 revertants/plate. See legend of Figure 1 for details. In the presence of methanol as a solvent control (A), the number of NNK-induced revertants was 80 revertants/plate.

Metabolic activation of NNK by mouse CYP2As expressed in S.typhimurium YG7108

To determine which one of the mouse CYP2A forms is responsible for the mutagenic activation of NNK, we

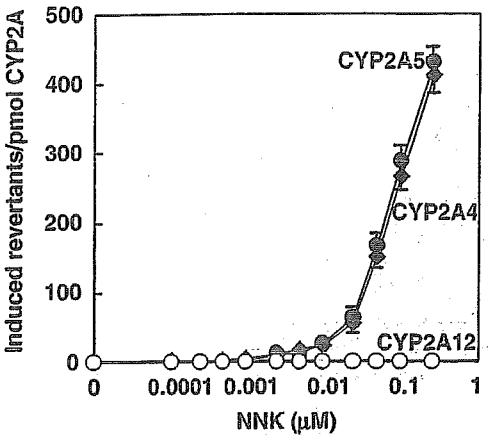

Fig. 3. Mutagenic activation of NNK by CYP2A4, CYP2A5 and CYP2A12 expressed in *S.typhimurium* YG7108 cells. NNK (0.1–250 nM) was exposed to *S.typhimurium* YG7108 cells expressing a mouse CYP2A. Closed diamond, closed circle and open circle represent the results with *S.typhimurium* YG7108 cells expressing CYP2A4, CYP2A5 and CYP2A12, respectively. Each value and bar indicates the mean and SD (range) of duplicate determinations, respectively.

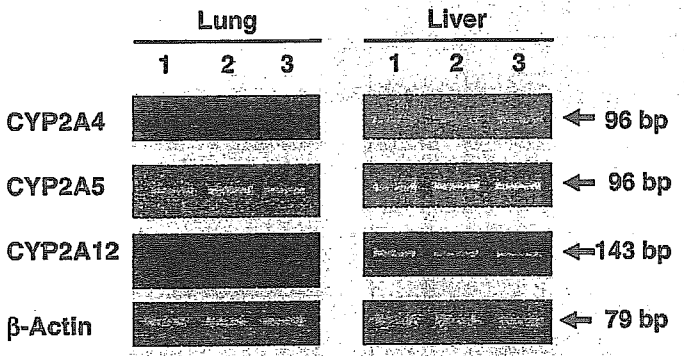

Fig. 4. Expression levels of mRNAs for CYP2A4, CYP2A5 and CYP2A12 in mouse lungs. Total RNA was prepared from lungs and livers of female mice. The expression of mRNAs for CYP2A4, CYP2A5 and CYP2A12 in the mouse lung or liver was determined by RT–PCR as described in Materials and methods. The sequence of specific primers for the mouse CYP2As is also described under Materials and methods. One tenth of each PCR solution was applied and separated in a 2% agarose ethidium bromide-stained gel. Each lane represents three individual samples.

performed the mutation assays using the genetically engineered *S.typhimurium* YG7108 each expressing CYP2A4, CYP2A5 or CYP2A12 together with CPR. As shown in Figure 3, CYP2A4 and CYP2A5, but not CYP2A12, was involved in the mutagenic activation of NNK. Apparent kinetic parameters for the mutagenic activation of NNK by CYP2A4 and CYP2A5 were calculated from the standard Michaelis–Menten velocity equation. Apparent K_m and V_{max} values for the activation by CYP2A4 and CYP2A5 were estimated to be 0.17 ± 0.03 μM and 770 induced revertants/pmol CYP2A4/μM and 0.18 ± 0.04 μM and 750 induced revertants/pmol CYP2A5/μM, respectively. Thus, both CYP2A forms showed similar apparent V_{max}/K_m values (4500 for CYP2A4 and 4200 for CYP2A5).

However, examination for the expression of CYP2As in mouse lung by RT–PCR indicated that mRNA for CYP2A5, but not for CYP2A4, was expressed, as shown in Figure 4. Taken together, these results suggested that CYP2A5 was a principal enzyme responsible for the mutagenic activation of NNK in the mouse lung.

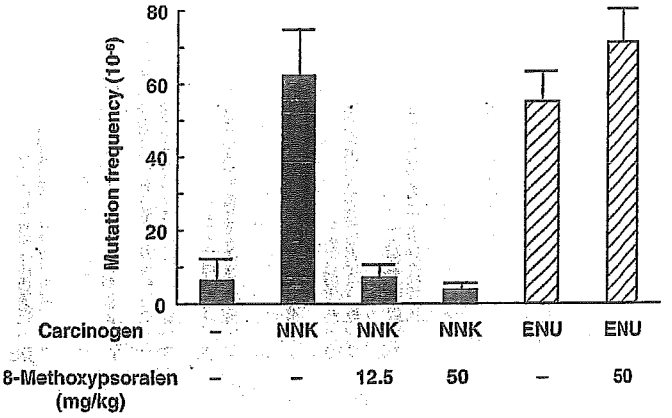

Fig. 5. 8-Methoxypsoralen inhibits the NNK-induced, but not ENU-induced, mutation of the *gpt delta* gene of the lung of *gpt delta* transgenic mice. Mice were pretreated with 8-methxypsoralen at a dose of 12.5 or 50 mg/kg body wt per oral or an equal amount of corn oil as a vehicle control with a stomach tube daily for 7 days. One h after treatment of mice with 8-methxypsoralen on day 3, each animal was treated with NNK or ENU at a dose of 100 mg/kg body wt, i.p. or equal volume of saline once daily for 4 days. The experiment was terminated on day 14 after the final NNK treatment. Each value and bar indicates the mean and SD (range) of duplicate determinations, respectively.

Effects of 8-methoxypsoralen on in vivo mutation caused by NNK in the gpt delta transgenic mice

To elucidate the role of mouse CYP2A in NNK-induced *in vivo* mutagenesis, we assessed the effects of 8-methoxypsoralen against NNK-induced mutation by using the transgenic mice carrying the *gpt delta* gene as a monitor of mutation. Oral feeding of 8-methoxypsoralen did not result in any apparent toxic effects even at a high concentration of 8-methoxypsoralen (100 mg/kg). No significant change was seen in food and water consumption and body wt (data not shown). As shown in Figure 5, the frequency of spontaneous mutation in the *gpt delta* gene in the lung was 6.4×10^{-6}. A single i.p. injection of NNK resulted in a 10-fold higher frequency of mutation (62.2×10^{-6}). The NNK-induced mutations in the lung were reduced by 89 and 94% when mice were pretreated with 8-methoxypsoralen at a dose of 12.5 or 50 mg/kg, respectively, prior to NNK. On the other hand, pretreatment of mice with 8-methoxypsoralen did not reduce ENU (a direct mutagen)-induced mutation whereas treatment of mice with ENU resulted in a 9-fold higher frequency of mutation (55.0×10^{-6}) in the *gpt* gene of the lung.

Effects of 8-methoxypsoralen on the NNK-induced lung tumors in A/J mice

As described previously, our previous study had demonstrated that pretreatment of female A/J mice with 8-methoxypsoralen strongly inhibited NNK-induced lung tumorigenesis (33). Here, we further investigated the inhibitory effects of 8-methoxypsoralen on the NNK-induced lung tumorigenesis. Lung whitish nodules were readily detected in the group of mice treated with NNK alone macroscopically but were rare in the group of mice treated with 8-methoxypsoralen alone and the group of mice pretreated with 12.5 mg/kg of 8-methoxypsoralen + NNK (Table I). Lung carcinoma could not be seen in any of the animals. Numbers and/or incidence of macroscopically observed lung nodules induced by NNK were reduced by 8-methoxyapsoralen in a dose-dependent manner ($P < 0.01$). The numbers of tumors/mouse were reduced from

21.04 (NNK alone) to 17.05, 7.89 and 1.25 by 0.125, 1.25 and 12.5 mg/kg body wt of 8-methoxyapsoralen, respectively, with the inhibitions by the latter two doses being statistically significant ($P < 0.01$).

The multiplicities and incidence of lung hyperplasias and adenomas are also summarized in Table I. Numbers and/or incidence of microscopically observed adenoma and hyperplasia induced by NNK were also reduced by 8-methoxypsoralen in a dose-dependent manner. Numbers of adenoma and hyperplasia were reduced from 15.61 (NNK alone) to 11.90, 5.44 and 1.15 by 0.125, 1.25 and 12.5 mg/kg body wt of 8-methoxypsoralen, respectively (Table I). Similarly, adenoma numbers were reduced from 13.44 to 10.25, 4.44 and 0.85 by 0.125, 1.25 and 12.5 mg/kg body wt of 8-methoxypsoralen, respectively, with the inhibitions by the latter two doses being statistically significant ($P < 0.01$).

To examine the mechanism(s) for the suppression of the NNK-induced lung tumorigenesis by 8-methoxypsoralen, we determined whether or not treatment of mice with 8-methoxypsoralen after the administration of NNK also inhibited the NNK-induced lung tumorigenesis. As shown in Table II, pretreatment of mice with 8-methoxypsoralen inhibited the incidence and multiplicities of macroscopically and microscopically examined lung lesions. However, treatment with 8-methoxypsoralen on days 1, 3 and 7 after NNK administration did not affect the incidence and multiplicities of examined lung lesions, suggesting that 8-methoxypsoralen abolished NNK-induced lung tumorigenesis via the inhibition of initiation event in carcinogenesis but not subsequent events including promotion and progression in carcinogenesis.

Expression of CYP2A in mouse lung adenomas induced by NNK

It was of interest to know if CYP2As were expressed in the region of NNK-induced lung lesions. Thus, we performed immunohistochemical examination for the expression of CYP2A using rabbit polyclonal anti-rat CYP2A1 antiserum in paraffin-embedded tumors containing NNK-induced lung adenomas. As shown in Figure 6, the expression of a protein(s) cross-reactive to antibodies to CYP2A1 was clearly seen in the region of NNK-induced lung tumor. Together with the data shown in Figure 3, it seemed possible to assume that CYP2A5 protein was expressed in the region of NNK-induced lung adenomas.

Discussion

The lung is one of the major target organs for NNK-induced tumor formation in laboratory animals including mice, rats and hamsters, regardless of the route of administration (1). A number of reports have appeared to date indicating that P450 is responsible for the metabolic activation of NNK (1,33,41–44). P450 forms belonging to the CYP2A subfamily have been studied in rats (CYP2A1, CYP2A2 and CYP2A3), mice (CYP2A4 and CYP2A5) and hamsters (CYP2A8, CYP2A9 and CYP2A16). CYP2As from these laboratory animals differ markedly in catalytic specificity despite similarity in their amino acid sequences (~70–90%) (45–50). In the present study, among mouse CYP2As, recombinant CYP2A4 and CYP2A5 activated NNK efficiently at nM concentrations of NNK in the mutation assays using the *S.typhimurium* YG7108, each expressing a form of the mouse CYP2A along with CPR (Figure 3). To our knowledge, the mutagenicity of *N*-nitrosamines including NNK at the nM level could not be detected in other studies reported so far. Furthermore, in our preliminary study, rat CYP2A3 and hamster CYP2A16 also activated NNK at nM levels of NNK using our genetically engineered *S.tyhimurium* YG7108 expressing a CYP2A. Collectively, these data may suggest that CYP2A subfamily member(s) play an important role in the mutagenic activation of NNK.

The mutagenic activation of NNK by mouse liver and lung microsomes was also inhibited by anti-CYP2A1 antibodies (Figures 1B and 2B). Since 8-methoxypsoralen is reported to inhibit CYP2A5 and human CYP2A6-mediated coumarin 7-hydroxylation, it has been recognized as a representative inhibitor of CYP2A5 and CYP2A6 (31,51,52). It has also been shown that 8-methoxypsoralen is a substrate for CYP2A6 and that the enzyme inhibition is due to competitive interaction (53,54). The metabolism-dependent inactivation of CYP2A6 by 8-methoxypsoralen has been shown to occur at low concentrations and at high rates (54). Using the *S.typhimurium* YG7108 expressing high levels of mouse or human CYP2A, 8-methoxypsoralen inhibited the metabolic activation of NNK (IC_{50} values were 0.039–0.66 μM) (unpublished data). The results of the present study provided strong evidence that the suppression by 8-methoxypsoralen, a typical CYP2A inhibitor, of NNK-induced lung tumorigenesis in mice can be explained by the inhibitory effects of 8-methoxypsoralen on the mutagenic activation of NNK catalyzed by CYP2A5 in the target organ in the initiation events of carcinogenesis.

von Pressentin *et al.* (55) have also reported that the administration of NNK in drinking water resulted in an increased mutation frequency in the organ including the lung of the *lacZ* mice (Muta™Mouse). In the present study, NNK-induced mutations in the lung of *gpt delta* transgenic mouse were almost completely abolished when mice were pretreated with 8-methoxypsoralen at a dose of 12.5 mg/kg. On the other hand, pretreatment of mice with 8-methoxypsoralen did not reduce the ENU (a direct mutagen)-induced mutation, suggesting that 8-methoxypsoralen might reduce the NNK-induced gene mutation via the inhibition of metabolic activation of NNK. Our preliminary DNA microarray analyses using the lungs from 8-methoxypsoralen and/or NNK-treated mice have shown that treatment with 8-methoxypsoralen and/or NNK did not alter the expression levels of P450s, phase II enzymes and DNA repair enzymes at 1 day after the treatment (unpublished data), when the metabolic activation of NNK had been reported to be almost completely finished (56). The expression of mRNA for CYP2A5, but not for CYP2A4, in the lung from untreated mice (Figure 4) and CYP2A proteins cross-reactive to anti-CYP2A1 antibodies seen in mouse lung adenoma induced by NNK (Figure 6) probably suggested that 8-methoxypsoralen inhibited further occurrence of mutation in the adenomas induced by NNK.

Treatment of mice with 8-methxypsoralen after NNK administration did not affect the incidence and multiplicities of lung lesions (Table II), probably suggesting that antimutagenic activity of 8-methoxypsoralen against NNK-induced mutation in an initiation event in carcinogenesis is a key step in the chemoprevention of this compound against NNK-induced lung tumorigenesis in mice. We also reported that CYP2A6 was capable of activating betel quid-specific *N*-nitrosamines (57) and that the *CYP2A6* gene deletion reduced oral cancer risk in betel quid chewers in Sri Lanka (58). Taken together with the data of this study, it is reasonable

Table I. Effects of treatment of female A/J mice with 8-methoxypsoralen prior to NNK on NNK-induced lung tumorigenesis

Group	NNK	8-Methoxypsoralen (mg/kg)	No.[a]	Macroscopical lung lesion		Hyperplasia		Adenoma		Hyperplasia and adenoma	
				Incidence (%)[b]	Whitish nodule/mouse[c]	Incidence (%)[b]	Tumors/mouse[c]	Incidence (%)[b]	Tumors/mouse[c]	Incidence (%)[b]	Tumors/mouse[c]
1	−	12.5	20	5/20 (25)	0.25 ± 0.44	1/20 (5)	0.05 ± 0.22	1/20 (5)	0.05 ± 0.93	2/20 (10)	0.10 ± 0.31
2	+	—	23	23/23 (100)	21.04 ± 12.56	18/23 (78)	2.17 ± 1.95	23/23 (100)	13.44 ± 7.94	23/23 (100)	15.61 ± 8.47
3	+	0.125	20	20/20 (100)	17.05 ± 15.24	14/20 (70)	1.65 ± 1.60	20/20 (100)	10.25 ± 7.87	20/20 (100)	11.90 ± 8.92
4	+	1.25	18	18/18 (100)	7.89 ± 2.63[d]	11/18 (61)	1.00 ± 0.97	18/18 (100)	4.44 ± 1.82[d]	18/18 (90)	5.44 ± 2.12[d]
5	+	12.5	20	12/20 (60)[e]	1.25 ± 1.29[d]	6/20 (30)[e]	0.30 ± 0.47	12/20 (60)[e]	0.85 ± 0.93[d]	14/20 (70)[e]	1.15 ± 1.04[d]

NNK (100 mg/kg) was injected i.p. to mice as described in Materials and methods.
[a]Number of mice examined.
[b]Number of mice with lesion (%).
[c]Mean ± SD.
[d]Significantly different from Group 2 by Student's *t*-test ($P < 0.01$).
[e]Significantly different from Group 2 by Fisher's exact probability test ($P < 0.01$).

Table II. Effects of treatment of female A/J mice with 8-methoxypsoralen before or after the administration of NNK on NNK-induced lung tumorigenesis

Group	NNK	8-Methoxypsoralen (mg/kg)	No.[a]	Macroscopical lung lesion		Hyperplasia		Adenoma		Hyperplasia and adenoma	
				Incidence (%)[b]	Whitish nodule/mouse[c]	Incidence (%)[b]	Tumors/ mouse[c]	Incidence (%)[b]	Tumors/mouse[c]	Incidence (%)[b]	Tumors/mouse[c]
1	−	Alone	19	3/19 (16)	0.16 ± 0.38	0/19 (0)	0	2/19 (11)	0.11 ± 0.32	2/19 (11)	0.11 ± 0.32
2	+	—	20	19/20 (95)	3.70 ± 3.06	9/20 (45)	0.75 ± 1.07	18/20 (90)	2.75 ± 2.10	19/20 (95)	3.50 ± 2.42
3	+	Pretreatment	20	9/20 (45)[d]	0.95 ± 1.54[e]	4/20 (20)	0.50 ± 1.15	8/20 (40)[d]	0.60 ± 0.88[e]	8/20 (40)[d]	1.10 ± 1.80[e]
4	+	1 day after NNK	19	17/19 (90)	4.26 ± 2.98	11/19 (58)	1.00 ± 1.15	17/19 (90)	3.00 ± 1.73	17/19 (90)	4.00 ± 2.45
5	+	3 days after NNK	20	20/20 (100)	3.70 ± 1.84	10/20 (50)	0.50 ± 0.51	19/20 (95)	3.05 ± 1.96	20/20 (100)	3.55 ± 2.01
6	+	7 days after NNK	20	19/20 (95)	3.10 ± 1.71	8/20 (40)	0.40 ± 0.50	19/20 (95)	2.65 ± 1.73	20/20 (100)	3.05 ± 1.79

NNK (100 mg/kg) was injected i.p. into mice.
[a]Number of mice examined.
[b]Number of mice with lesion (%).
[c]Mean ± SD.
[d]Significantly different from Group 2 by Fisher's exact probability test ($P < 0.01$).
[e]Significantly different from Group 2 by Student's *t*-test ($P < 0.005$).

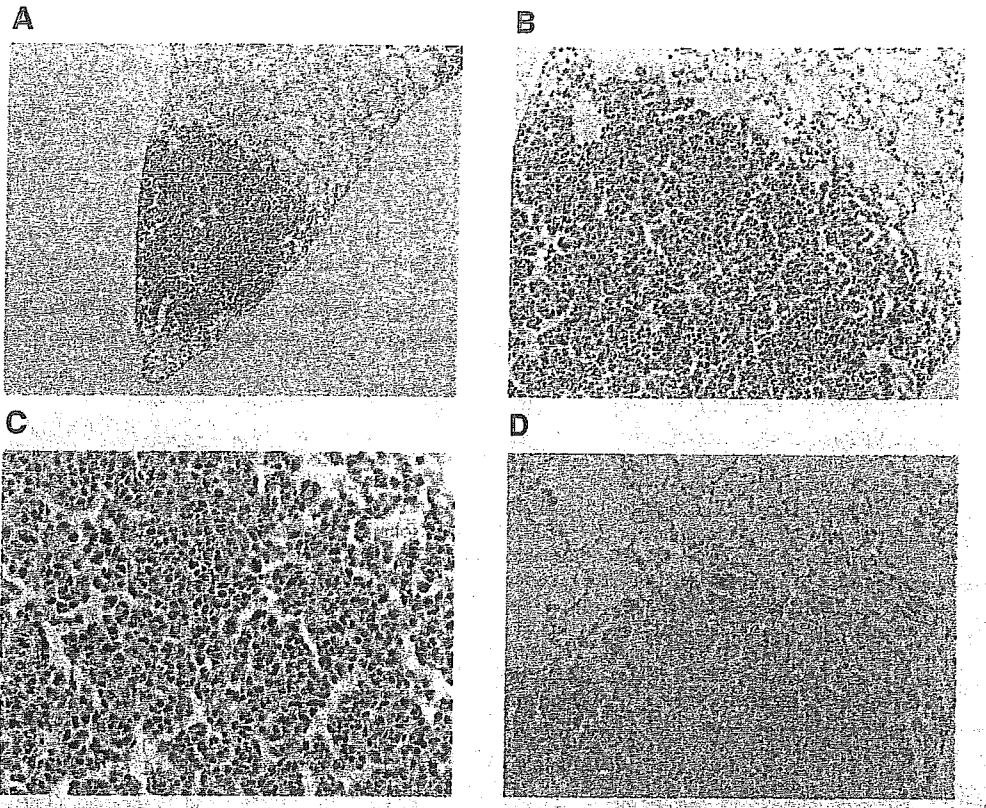

Fig. 6. Immunohistochemical examination for the expression of CYP2A in adenoma induced by NNK in the mouse lung. The boundary of the lesion was usually well demarcated. The paraffin-embedded lung sections were immunostained with rabbit polyclonal anti-rat CYP2A1 antibodies (A–C) or preimmune (D). A, B and D, and C display lung adenomas at 40×, 100× and 200× magnifications, respectively.

to assume that the function of CYP2A6 as an initial event in carcinogenesis plays an important role in lung cancer caused by smoking. In accordance with this idea, we demonstrated in a previous report that the function of CYP2A6 evaluated from *CYP2A6* genetic polymorphisms is a key determinant of tobacco-related lung cancer risk in male Japanese smokers (26).

In conclusion, the results of this study indicate for the first time that 8-methoxypsoralen prevents NNK-induced lung mutagenesis and tumorigenesis in mice by inhibition of CYP2A5 in the lung.

Acknowledgements

This work was supported, in part, by the Ministry of Education, Science, Sports and Culture of Japan and by a Grant-in-Aid from the Ministry of Health, Labor and Welfare of Japan. This work was also supported, in part, by a Grant-in-Aid (No. 99-2) from the Organization for Pharmaceutical Safety and Research (OPSR) and an SRF Grant for Biomedical Research in Japan.

Conflict of Interest Statement: None declared.

References

1. Hecht,S.S. (1998) Biochemistry, biology, and carcinogenicity of tobacco-specific *N*-nitrosamines. *Chem. Res. Toxicol.*, **11**, 559–603.
2. Hoffmann,D. and Hoffmann,I. (1997) The changing cigarette, 1950–1995. *J. Toxicol. Environ. Health*, **50**, 307–364.
3. Hecht,S.S. (1999) Tobacco smoke carcinogens and lung cancer. *J. Natl Cancer Inst.*, **91**, 1194–1210.
4. Hecht,S.S. (2002) Cigarette smoking and lung cancer: chemical mechanisms and approaches to prevention. *Lancet Oncol.*, **3**, 461–469.
5. Crespi,C.L., Penman,B.W., Gelboin,H.V. and Gonzalez,F.J. (1991) A tobacco smoke-derived nitrosamine, 4-(methylnitrosamino)-1-(3-pyridyl)-1-butanone, is activated by multiple human cytochrome P450s including the polymorphic human cytochrome P4502D6. *Carcinogenesis*, **12**, 1197–1201.
6. Peterson,L.A. and Hecht,S.S. (1991) O^6-methylguanine is a critical determinant of 4-(methylnitrosamino)-1-(3-pyridyl)-1-butanone tumorigenesis in A/J mouse lung. *Cancer Res.*, **51**, 5557–5564.
7. Ronai,Z.A., Gradia,S., Peterson,L.A. and Hecht,S.S. (1993) G to A transitions and G to T transversions in codon 12 of the *Ki-ras* oncogene isolated from mouse lung tumors induced by 4-(methylnitrosamino)-1-(3-pyridyl)-1-butanone (NNK) and related DNA methylating and pyridyloxobutylating agents. *Carcinogenesis*, **14**, 2419–2422.
8. Porter,T.D. and Coon,M.J. (1991) Cytochrome P-450. Multiplicity of isoforms, substrates, and catalytic and regulatory mechanisms. *J. Biol. Chem.*, **266**, 13469–13472.
9. Nelson,D.R., Kamataki,T., Waxman,D.J., Guengerich,F.P., Estabrook,R.W., Feyereisen,R., Gonzalez,F.J., Coon,M.J., Gunsalus,I.C., Gotoh,O., Okuda,K. and Nebert,D.W. (1993) The P450 superfamily: update on new sequences, gene mapping, accession numbers, early trivial names of enzymes, and nomenclature. *DNA Cell. Biol.*, **12**, 1–51.
10. Nelson,D.R., Koymans,L., Kamataki,T., Stegeman,J.J., Feyereisen,R., Waxman,D.J., Waterman,M.R., Gotoh,O., Coon,M.J., Estabrook,R.W., Gunsalus,I.C. and Nebert,D.W. (1996) P450 superfamily: update on new sequences, gene mapping, accession numbers and nomenclature. *Pharmacogenetics*, **6**, 1–42.
11. Guengerich,F.P. and Shimada,T. (1991) Oxidation of toxic and carcinogenic chemicals by human cytochrome P-450 enzymes. *Chem. Res. Toxicol.*, **4**, 391–407.
12. Guengerich,F.P. (2001) Common and uncommon cytochrome P450 reactions related to metabolism and chemical toxicity. *Chem. Res. Toxicol.*, **14**, 611–650.
13. Yamano,S., Nagata,K., Yamazoe,Y., Kato,R., Gelboin,H.V. and Gonzalez,F.J. (1989) cDNA and deduced amino acid sequences of human P450 IIA3 (CYP2A3). *Nucleic Acids Res.*, **17**, 4888.
14. Mace,K., Bowman,E.D., Vautravers,P., Shields,P.G., Harris,C.C. and Pfeifer,A.M. (1998) Characterisation of xenobiotic-metabolising enzyme

expression in human bronchial mucosa and peripheral lung tissues. *Eur. J. Cancer*, **34**, 914–920.
5. Crawford,E.L., Weaver,D.A., DeMuth,J.P., Jackson,C.M., Khuder,S.A., Frampton,M.W., Utell,M.J., Thilly,W.G. and Willey,J.C. (1998) Measurement of cytochrome P450 2A6 and 2E1 gene expression in primary human bronchial epithelial cells. *Carcinogenesis*, **19**, 1867–1871.
6. Yamazaki,H., Inui,Y., Yun,C.H., Guengerich,F.P. and Shimada,T. (1992) Cytochrome P450 2E1 and 2A6 enzymes as major catalysts for metabolic activation of *N*-nitrosodialkylamines and tobacco-related nitrosamines in human liver microsomes. *Carcinogenesis*, **13**, 1789–1794.
7. Kushida,H., Fujita,K., Suzuki,A., Yamada,M., Endo,T., Nohmi,T. and Kamataki,T. (2000) Metabolic activation of *N*-alkylnitrosamines in genetically engineered *Salmonella typhimurium* expressing CYP2E1 or CYP2A6 together with human NADPH-cytochrome P450 reductase. *Carcinogenesis*, **21**, 1227–1232.
8. Fernandez-Salguero,P., Hoffman,S., Cholerton,S., Mohrenweiser,H., Raunio,H., Rautio,A., Pelkonen,O., Huang,J., Evans,W., Idle,J. and Gonzalez,F.J. (1995) A genetic polymorphism in coumarin 7-hydroxylation: sequence of the human CYP2A genes and identification of variant CYP2A6 alleles. *Am. J. Hum. Genet.*, **57**, 651–660.
9. Ujjin,P., Satarug,S., Vanavanitkun,Y., Daigo,S., Ariyoshi,N., Yamazaki,H., Reilly,P.E., Moore,M.R. and Kamataki,T. (2002) Variation in coumarin 7-hydroxylase activity associated with genetic polymorphism of cytochrome P450 2A6 and the body status of iron stores in adult Thai males and females. *Pharmacogenetics*, **12**, 241–249.
10. Nunoya,K., Yokoi,T., Kimura,K., Inoue,K., Kodama,T., Funayama,M., Nagashima,K., Funae,Y., Green,C., Kinoshita,M. and Kamataki,T. (1998) A new deleted allele in the human cytochrome P450 2A6 (CYP2A6) gene found in individuals showing poor metabolic capacity to coumarin and (+)-*cis*-3,5-dimethyl-2-(3-pyridyl)thiazolidin-4-one hydrochloride (SM-12502). *Pharmacogenetics*, **8**, 239–249.
11. Nunoya,K.I., Yokoi,T., Kimura,K., Kainuma,T., Satoh,K., Kinoshita,M. and Kamataki,T. (1999) A new *CYP2A6* gene deletion responsible for the *in vivo* polymorphic metabolism of (+)-*cis*-3,5-dimethyl-2-(3-pyridyl)thiazolidin-4-one hydrochloride in humans. *J. Pharmacol. Exp. Ther.*, **289**, 437–442.
12. Ariyoshi,N., Sawamura,Y. and Kamataki,T. (2001) A novel single nucleotide polymorphism altering stability and activity of *CYP2A6*. *Biochem. Biophys. Res. Commun.*, **281**, 810–814.
13. Daigo,S., Takahashi,Y., Fujieda,M., Ariyoshi,N., Yamazaki,H., Koizumi,W., Tanabe,S., Nagayama,S., Ikeda,K., Nishioka,Y. and Kamataki,T. (2002) A novel mutant allele of the *CYP2A6* gene (*CYP2A6*11*) found in a cancer patient who showed poor metabolic phenotype towards tegafur. *Pharmacogenetics*, **12**, 299–306.
14. Miyamoto,M., Umetsu,Y., Dosaka-Akita,H., Sawamura,Y., Yokota,J., Kunitoh,H., Nemoto,N., Sato,K., Ariyoshi,N. and Kamataki,T. (1999) *CYP2A6* gene deletion reduces susceptibility to lung cancer. *Biochem. Biophys. Res. Commun.*, **261**, 658–660.
15. Ariyoshi,N., Miyamoto,M., Umetsu,Y., Kunitoh,H., Dosaka-Akita,H., Sawamura,Y., Yokota,J., Nemoto,N., Sato,K. and Kamataki,T. (2002) Genetic polymorphism of *CYP2A6* gene and tobacco-induced lung cancer risk in male smokers. *Cancer Epidemiol. Biomarkers Prev.*, **11**, 890–894.
16. Fujieda,M., Yamazaki,H., Saito,T., Kiyotani,K., Gyamfi,M., Sakurai,M., Dosaka-Akita,H., Sawamura,Y., Yokota,J., Kunitoh,H. and Kamataki,T. (2004) Evaluation of *CYP2A6* genetic polymorphisms as determinants of smoking behavior and tobacco-related lung cancer risk in male Japanese smokers. *Carcinogenesis*, **25**, 2451–2458.
17. Scott,B.R., Pathak,M.A. and Mohn,G.R. (1976) Molecular and genetic basis of furocoumarin reactions. *Mutat. Res.*, **39**, 29–74.
18. Melski,J.W., Tanenbaum,L., Parrish,J.A., Fitzpatrick,T.B. and Bleich,H.L. (1977) Oral methoxsalen photochemotherapy for the treatment of psoriasis: a cooperative clinical trial. *J. Invest. Dermatol.*, **68**, 328–335.
19. Parrish,J.A., Fitzpatrick,T.B., Tanenbaum,L. and Pathak,M.A. (1974) Photochemotherapy of psoriasis with oral methoxsalen and longwave ultraviolet light. *N. Engl. J. Med.*, **291**, 1207–1211.
20. Koenigs,L.L., Peter,R.M., Thompson,S.J., Rettie,A.E. and Trager,W.F. (1997) Mechanism-based inactivation of human liver cytochrome P450 2A6 by 8-methoxypsoralen. *Drug Metab. Dispos.*, **25**, 1407–1415.
21. Maenpaa,J., Sigusch,H., Raunio,H., Syngelma,T., Vuorela,P., Vuorela,H. and Pelkonen,O. (1993) Differential inhibition of coumarin 7-hydroxylase activity in mouse and human liver microsomes. *Biochem. Pharmacol.*, **45**, 1035–1042.
22. Yamazaki,H., Mimura,M., Sugahara,C. and Shimada,T. (1994) Catalytic roles of rat and human cytochrome P450 2A enzymes in testosterone 7α- and coumarin 7-hydroxylations. *Biochem. Pharmacol.*, **48**, 1524–1527.
23. Takeuchi,H., Saoo,K., Yokohira,M., Ikeda,M., Maeta,H., Miyazaki,M., Yamazaki,H., Kamataki,T. and Imaida,K. (2003) Pretreatment with 8-methoxypsoralen, a potent human CYP2A6 inhibitor, strongly inhibits lung tumorigenesis induced by 4-(methylnitrosamino)-1-(3-pyridyl)-1-butanone in female A/J mice. *Cancer Res.*, **63**, 7581–7583.
24. Fujita Ki,K., Nakayama,K., Yamazaki,Y., Tsuruma,K., Yamada,M., Nohmi,T. and Kamataki,T. (2001) Construction of *Salmonella typhimurium* YG7108 strains, each coexpressing a form of human cytochrome P450 with NADPH-cytochrome P450 reductase. *Environ. Mol. Mutagen.*, **38**, 329–338.
25. Omura,T. and Sato,R. (1964) The carbon monoxide-binding pigment of liver microsomes. I. Evidence for its hemoprotein nature. *J. Biol. Chem.*, **239**, 2379–2385.
26. Phillips,A.H. and Langdon,R.G. (1962) Hepatic triphosphopyridine nucleotide (TPN)-cytochrome *c* reductase: isolation, characterization and kinetic studies. *J. Biol. Chem.*, **237**, 2652–2660.
27. Maron,D.M. and Ames,B.N. (1983) Revised methods for the Salmonella mutagenicity test. *Mutat. Res.*, **113**, 173–215.
28. Guengerich,F. (1994) Analysis and characterization of enzyme. In: Hayes,A.W. (ed.), *Principles and Methods of Toxicology*. Raven Press, NY, pp. 1259–1313.
29. Nohmi,T., Katoh,M., Suzuki,H., Matsui,M., Yamada,M., Watanabe,M., Suzuki,M., Horiya,N., Ueda,O., Shibuya,T., Ikeda,H. and Sofuni,T. (1996) A new transgenic mouse mutagenesis test system using Spi- and 6-thioguanine selections. *Environ. Mol. Mutagen.*, **28**, 465–470.
30. Rehm,S., Word,J. and Sass,B. (1994) Tumors of the lungs. In: Turusov,V.S. and Mohrs,U. (eds), *Pathology of Tumors in Laboratory Animals*, Vol. 2, Tumours of the Mouse. Lyon, pp. 325–355.
31. Smith,T.J., Guo,Z.Y., Thomas,P.E., Chung,F.L., Morse,M.A., Elkind,K. and Yang,C.S. (1990) Metabolism of 4-(methylnitrosamino)-1-(3-pyridyl)-1-butanone in mouse lung microsomes and its inhibition by isothiocyanates. *Cancer Res.*, **50**, 6817–6822.
32. Guo,Z., Smith,T.J., Thomas,P.E. and Yang,C.S. (1991) Metabolic activation of 4-(methylnitrosamino)-1-(3-pyridyl)-1-butanone as measured by DNA alkylation *in vitro* and its inhibition by isothiocyanates. *Cancer Res.*, **51**, 4798–4803.
33. Smith,T.J., Guo,Z., Gonzalez,F.J., Guengerich,F.P., Stoner,G.D. and Yang,C.S. (1992) Metabolism of 4-(methylnitrosamino)-1-(3-pyridyl)-1-butanone in human lung and liver microsomes and cytochromes P-450 expressed in hepatoma cells. *Cancer Res.*, **52**, 1757–1763.
34. Smith,T.J., Guo,Z., Hong,J.Y., Ning,S.M., Thomas,P.E. and Yang,C.S. (1992) Kinetics and enzyme involvement in the metabolism of 4-(methylnitrosamino)-1-(3-pyridyl)-1-butanone (NNK) in microsomes of rat lung and nasal mucosa. *Carcinogenesis*, **13**, 1409–1414.
35. Burkhart,B.A., Harada,N. and Negishi,M. (1985) Sexual dimorphism of testosterone 15 alpha-hydroxylase mRNA levels in mouse liver. cDNA cloning and regulation. *J. Biol. Chem.*, **260**, 15357–15361.
36. Kaipainen,P., Nebert,D.W. and Lang,M.A. (1984) Purification and characterization of a microsomal cytochrome P-450 with high activity of coumarin 7-hydroxylase from mouse liver. *Eur. J. Biochem.*, **144**, 425–431.
37. Juvonen,R.O., Shkumatov,V.M. and Lang,M.A. (1988) Purification and characterization of a liver microsomal cytochrome P-450 isoenzyme with a high affinity and metabolic capacity for coumarin from pyrazole-treated D2 mice. *Eur. J. Biochem.*, **171**, 205–211.
38. Iwasaki,M., Lindberg,R.L., Juvonen,R.O. and Negishi,M. (1993) Site-directed mutagenesis of mouse steroid 7 alpha-hydroxylase (cytochrome P-450(7) alpha): role of residue-209 in determining steroid-cytochrome P-450 interaction. *Biochem. J.*, **291**, 569–573.
39. Lindberg,R., Burkhart,B., Ichikawa,T. and Negishi,M. (1989) The structure and characterization of type I *P-450*$15_{15\alpha}$ gene as major steroid 15 alpha-hydroxylase and its comparison with type II *P-450*$15_{15\alpha}$ gene. *J. Biol. Chem.*, **264**, 6465–6471.
40. Honkakoski,P. and Negishi,M. (1997) The structure, function, and regulation of cytochrome P450 2A enzymes. *Drug Metab. Rev.*, **29**, 977–996.
41. Szutowski,M., Lukasik,M., Wawer,Z., Chrobak,K., Michalska,M., Borzecka,K. and Brzezinski,J. (2002) *In vivo* effect of 5- and 8-methoxypsoralens and cimetidine on R,S-warfarin metabolism in rat. *J. Appl. Toxicol.*, **22**, 327–332.
42. Ono,S., Hatanaka,T., Hotta,H., Satoh,T., Gonzalez,F.J. and Tsutsui,M. (1996) Specificity of substrate and inhibitor probes for cytochrome P450s: evaluation of *in vitro* metabolism using cDNA-expressed human P450s and human liver microsomes. *Xenobiotica*, **26**, 681–693.
43. Draper,A.J., Madan,A. and Parkinson,A. (1997) Inhibition of coumarin 7-hydroxylase activity in human liver microsomes. *Arch. Biochem. Biophys.*, **341**, 47–61.

54. Kharasch,E.D., Hankins,D.C. and Taraday,J.K. (2000) Single-dose methoxsalen effects on human cytochrome P-450 2A6 activity. *Drug Metab. Dispos.*, **28**, 28–33.
55. von Pressentin,M.M., Chen,M. and Guttenplan,J.B. (2001) Mutagenesis induced by 4-(methylnitrosamino)-1-(3-pyridyl)-1-butanone-4-(methylnitrosamino)-1-(3-pyridyl)-1-butanone and N-nitrosonornicotine in *lacZ* upper aerodigestive tissue and liver and inhibition by green tea. *Carcinogenesis*, **22**, 203–206.
56. Castonguay,A., Tjalve,H. and Hecht,S.S. (1983) Tissue distribution of tobacco-specific carcinogen 4-(methylnitrosamino)-1-(3-pyridyl)-1-butanone (NNK) and its metabolites in F344 rats. *Cancer Res.*, **43**, 630–638.
57. Miyazaki,M., Sugawara,E., Yoshimura,T., Yamazaki,H. and Kamataki,T. (2005) Mutagenic activation of betel quid-specific *N*-nitrosamines catalyzed by human cytochrome P450 coexpressed with NADPH-cytochrome P450 reductase in *Salmonella typhimurium* YG7108. *Mutat. Res.*, **581**, 165–171.
58. Topcu,Z., Chiba,I., Fujieda,M., Shibata,T., Ariyoshi,N., Yamazaki,H., Sevgican,F., Muthumala,M., Kobayashi,H. and Kamataki,T. (2002) *CYP2A6* gene deletion reduces oral cancer risk in betel quid chewers in Sri Lanka. *Carcinogenesis*, **23**, 595–598.

Received April 2, 2005; revised June 4, 2005; accepted June 7, 2005

Oncogene (2005) 24, 1328–1337
© 2005 Nature Publishing Group All rights reserved 0950-9232/05 $30.00
www.nature.com/onc

Parp-1 deficiency causes an increase of deletion mutations and insertions/rearrangements *in vivo* after treatment with an alkylating agent

Atsushi Shibata[1,2,3], Nobuo Kamada[4], Ken-ichi Masumura[5], Takehiko Nohmi[5], Shizuko Kobayashi[2], Hirobumi Teraoka[3], Hitoshi Nakagama[1], Takashi Sugimura[1], Hiroshi Suzuki[4,6] and Mitsuko Masutani*[,1]

[1]*Biochemistry Division, National Cancer Center Research Institute, Chuo-ku, Tokyo, Japan;* [2]*Kyoritsu College of Pharmacy, Minato-ku, Tokyo, Japan;* [3]*Medical Research Institute, Tokyo Medical and Dental University, Chiyoda-ku, Tokyo, Japan;* [4]*Chugai Pharmaceutical Co. Ltd, Gotemba, Shizuoka, Japan;* [5]*Division of Genetics and Mutagenesis, National Institute of Health Sciences, Setagaya-ku, Tokyo, Japan*

Accumulated evidence suggests that Parp-1 is involved in DNA repair processes, including base excision repair, single-strand and double-strand break repairs. To understand the precise role of Parp-1 in genomic stability *in vivo*, we carried out mutation analysis using *Parp-1* knockout (*Parp-1*$^{-/-}$) mice harboring two marker genes, *gpt* and *red/gam* genes. Spontaneous mutant frequencies of both genes in the bone marrows and livers did not differ significantly between *Parp-1*$^{-/-}$ and *Parp-1*$^{+/+}$ mice ($P > 0.05$). After treatment with an alkylating agent, *N*-nitrosobis(2-hydroxypropyl)amine (BHP), the mutant frequency of the *red/gam* genes in the liver in *Parp-1*$^{-/-}$ mice was 1.6-fold higher than that in *Parp-1*$^{+/+}$ mice ($P < 0.05$). Categorization of the mutations revealed that deletions larger than 1 kb or those accompanying 1–5 bp insertions at the deletion junctions, as well as rearrangements, were more frequently observed in *Parp-1*$^{-/-}$ than in *Parp-1*$^{+/+}$ mice ($P < 0.05$, respectively). In contrast, mutant frequencies of the *gpt* gene in the livers of *Parp-1*$^{-/-}$ and *Parp-1*$^{+/+}$ mice after BHP treatment were both elevated and there was no significant difference between the genotypes. These results indicate that Parp-1 is implicated in suppressing deletion mutations *in vivo*, especially those accompanying small insertions or rearrangements.
Oncogene (2005) **24**, 1328–1337. doi:10.1038/sj.onc.1208289
Published online 20 December 2004

Keywords: Parp-1; *gpt* delta; deletion; mutation; recombination; rearrangement

Introduction

Poly(ADP-ribose) polymerase-1 (Parp-1) is activated by binding to single-strand break (SSB) and double-strand break (DSB) ends, and catalyses polyADP ribosylation of various nuclear proteins, including Parp-1 itself (Yoshihara *et al.*, 1977; Adolph and Song, 1985), histone (Buki *et al.*, 1995), p53 (Wesierska-Gadek *et al.*, 1996), and DNA-dependent protein kinase (DNA-PKcs) (Ariumi *et al.*, 1999) using NAD as a substrate. Parp-1 possesses a BRCT (BRCA1 C-terminal) motif being overlapped with an automodification domain, and binds to various proteins through this domain, including XRCC1 (Masson *et al.*, 1998), histone (Buki *et al.*, 1995), and Parp-2 (Schreiber *et al.*, 2002). Accumulating studies have indicated Parp-1 to be involved in base excision repair (BER) (Caldecott *et al.*, 1996a; Masson *et al.*, 1998), SSB (Okano *et al.*, 2003), and DSB repairs (Morrison *et al.*, 1997) through its enzymatic activity and/or protein–protein interaction through the BRCT domain.

In the BER reaction, cleavage of damaged bases takes place and, subsequently, SSB is introduced by the excision of abasic sites by nucleases. Parp-1 binds to SSB ends and is involved in the recruitment of XRCC1 (Caldecott *et al.*, 1996b; Masson *et al.*, 1998; El-Khamisy *et al.*, 2003), DNA polymerase β (pol β) (Caldecott *et al.*, 1996b; Masson *et al.*, 1998), and DNA ligase III (Leppard *et al.*, 2003). In the cell-free system, DNA polymerization by pol β and strand displacement by flap endonuclease-1 (FEN-1) in the long-patch repair is disturbed in the absence of Parp-1 (Vodenicharov *et al.*, 2000; Prasad *et al.*, 2001). Another study showed a decreased level of long-patch repair in *Parp-1*$^{-/-}$ cells, with reduction in the levels of FEN-1 and DNA ligase I (Sanderson and Lindahl, 2002).

DSB repair is categorized into homologous recombination (HR) repair and nonhomologous end joining (NHEJ) repair pathways. Involvement of Parp-1 in NHEJ repair has been also suggested from the interaction with DNA-PKcs and Ku70/80 (Ariumi *et al.*, 1999; Galande and Kohwi-Shigematsu, 1999). Parp-1 is also indicated to suppress HR repair, and the frequencies of gene-targeting (Waldman and Waldman, 1990; Semionov *et al.*, 1999, 2003; Susse *et al.*, 2004) and sister chromatid exchanges were increased in *Parp-1*$^{-/-}$ cells (de Murcia *et al.*, 1997; Wang *et al.*, 1997) and by treatment with Parp inhibitors (Oikawa *et al.*, 1980).

*Correspondence: M Masutani, Biochemistry Division, National Cancer Center Research Institute, 5-1-1, Chuo-ku, Tokyo, 104-0045 Japan; E-mail: mmasutan@gan2.res.ncc.go.jp
[6]Current address: National Research Center for Protozoan Diseases, Obihiro University of Agriculture and Veterinary Medicine, Obihiro, Hokkaido, Japan
Received 4 May 2004; revised 4 October 2004; accepted 7 October 2004; published online 20 December 2004

The involvement of Parp-1 in BER and DSB repair, and its suppressive role in HR repair, suggests that deletion or insertion mutations may accumulate under *Parp-1* deficiency. On the other hand, it is reported that the gene-targeting frequency was not different between *Parp-1*$^{-/-}$ and *Parp-1*$^{+/+}$ cells, and it is therefore suggested that Parp-1 is dispensable in NHEJ and HR induced by DSBs (Yang *et al.*, 2004).

Analysis of mutant frequencies and spectra in *Parp-1*$^{-/-}$ mice *in vivo* would be helpful to understand the impact of *Parp-1* deficiency on DNA repair and genomic stability. For this purpose, we established *Parp-1*$^{-/-}$ mice, harboring a tandem array of 80 copies of lambda EG10 DNA containing two surrogate marker genes by intercrossing with *gpt* delta transgenic mice (Nohmi *et al.*, 1996). Point mutations can be detected by *gpt* assay, and deletion mutations ranging from 1 bp up to 9.1 kbp are able to be efficiently identified in the *red/gam* genes by Spi$^-$ assay, as shown in Figure 1 (Masumura *et al.*, 1999; Nohmi *et al.*, 1999; Okada *et al.*, 1999).

In the present study, we analysed spontaneous mutations in the bone marrow and livers of *Parp-1*$^{-/-}$ and *Parp-1*$^{+/+}$ mice. Since *Parp-1*$^{-/-}$ mice show higher susceptibility to the lethality induced by alkylating agents (de Murcia *et al.*, 1997; Masutani *et al.*, 2000), and to the tumorigenicity of agents such as *N*-nitrosobis(2-hydroxypropyl)amine (BHP) and azoxymethane (Tsutsumi *et al.*, 2001; Nozaki *et al.*, 2003) compared to *Parp-1*$^{+/+}$ mice, we also analysed mutations after treatment with BHP. We demonstrated that the frequency of deletion mutations, but not point mutations, was higher in BHP-treated *Parp-1*$^{-/-}$ than in *Parp-1*$^{+/+}$ mice ($P<0.05$). Notably, larger size deletions and complex-type deletions accompanying small insertions or recombination/rearrangement were significantly increased in *Parp-1*$^{-/-}$ when compared to *Parp-1*$^{+/+}$ animals ($P<0.05$, respectively).

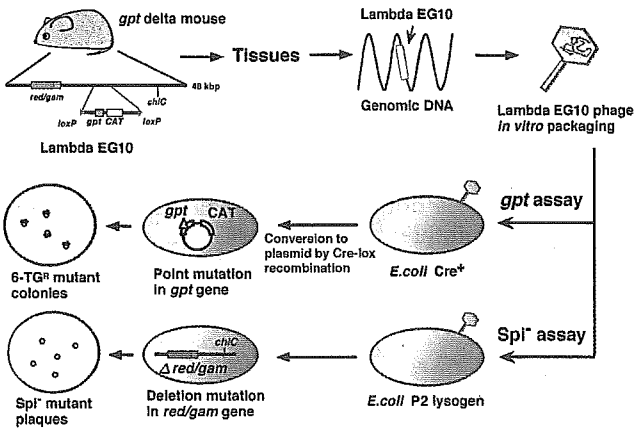

Figure 1 Scheme for *gpt* and Spi$^-$ assays for detecting mutations in gpt delta mice. The lambda EG10 phages are rescued from mouse genomic DNA by *in vitro* packaging. In *gpt* assay, lambda phages are infected into *E. coli* strain YG6020 expressing Cre recombinase and 6.4 kb region of lambda EG10, containing the *gpt* gene, was converted to plasmid. Mutation in *gpt* genes can be positively selected using a plate containing chloramphenicol and 6-TG. In Spi$^-$ assay, lambda phages are infected into *E. coli* harboring P2 lysogen. Lambda phages containing deletion mutations in *red/gam* genes can selectively grow and form Spi$^-$ mutant plaques

Results

Spontaneous mutations in the bone marrow of Parp-1$^{-/-}$ *mice*

In the *gpt* assay, which detects point mutations in the *gpt* gene (Figure 1), the spontaneous mutation frequencies of the bone marrow in *Parp-1*$^{+/+}$ and *Parp-1*$^{-/-}$ mice ($n=5$, respectively) were 6.9 ± 3.1 ($\times10^{-6}$), and 5.6 ± 1.2 ($\times10^{-6}$). There was no significant difference between *Parp-1*$^{+/+}$ and *Parp-1*$^{-/-}$ mice ($P=0.75$). The spectra and distribution patterns of the mutations in the *gpt* gene were not different between *Parp-1*$^{+/+}$ and *Parp-1*$^{-/-}$ mice (data not shown).

In the Spi$^-$ assay, which detects deletion mutations in the *red/gam* genes (Figure 1), mutant frequencies in *Parp-1*$^{-/-}$ and *Parp-1*$^{+/+}$ mice ($n=5$, respectively) were 8.0 ± 1.0 ($\times10^{-6}$) and 6.7 ± 2.0 ($\times10^{-6}$), respectively, and there was no significant difference between either genotype ($P=0.46$). The spectra and the distributions of the mutations in the *red/gam* genes were analysed with 39 and 27 mutants for *Parp-1*$^{-/-}$ and *Parp-1*$^{+/+}$ animals, respectively. Most of the mutations were deletion mutations of 1–6 bp at single-nucleotide run sequences and there was no difference in the distribution of mutation sites between the genotypes (data not shown).

Increase in Spi$^-$ mutant frequencies in the liver of BHP-treated Parp-1$^{-/-}$ *mice*

Genomic DNA was prepared from the liver, a major target organ of BHP (Green *et al.*, 1980). Mutant frequency of the *gpt* gene in the livers of nontreated mice ($n=4$) was 5.7 ± 0.9 ($\times10^{-6}$) and 10 ± 1.8 ($\times10^{-6}$) in *Parp-1*$^{+/+}$ and *Parp-1*$^{-/-}$ mice, respectively. After BHP treatment, mutant frequencies were increased to 89 ± 6.4 ($\times10^{-6}$) and 66 ± 12 ($\times10^{-6}$), respectively. There was no significant difference between the genotypes of the nontreated ($P=0.059$) and the BHP-treated mice ($P=0.083$) (see Supplementary Information).

Spi$^-$ mutant frequencies in nontreated *Parp-1*$^{+/+}$ and *Parp-1*$^{-/-}$ mice were not statistically different ($P=0.083$). On the other hand, Spi$^-$ mutant frequencies in BHP-treated mice increased to 16 ± 2.0 ($\times10^{-6}$) and 26 ± 4.2 ($\times10^{-6}$), respectively. The mutant frequency in *Parp-1*$^{-/-}$ mice was 1.6-fold higher compared with *Parp-1*$^{+/+}$ mice ($P<0.05$, Table 1).

Analysis of mutation spectrum

Mutation spectra of 83 and 179 Spi$^-$ mutant phages rescued from *Parp-1*$^{+/+}$ and *Parp-1*$^{-/-}$ mice, respectively, were analysed as shown in Table 2. Most of the Spi$^-$ mutations were deletions and the specific mutation frequencies of the total deletion mutations were 1.7-fold higher in *Parp-1*$^{-/-}$ than in *Parp-1*$^{+/+}$ mice, although the

Table 1 Mutant frequency of the *red/gam* genes in the livers of nontreated and BHP-treated mice

BHP	*Genotype*	*Mouse identification no.*	*Titer ($\times 10^6$)*	*No. of Spi⁻ mutant plaques*	*Mutant frequency ($\times 10^{-6}$)*	
						Mean±s.e.
Control	*Parp-1*$^{+/+}$	G27	3.03	20	6.6	7.5±1.0
		G28	1.29	7	5.4	
		G53	2.91	24	8.2	
		G89	1.94	19	9.8	
	Parp-1$^{-/-}$	G19	1.03	8	7.8	3.6±1.5
		G23	3.16	4	1.3	
		G29	3.46	5	1.4	
		G68	1.31	5	3.8	
2 g/kg body weight	*Parp-1*$^{+/+}$	G79	1.30	14	11	16±2.0
		G81	1.47	26	18	
		G82	1.31	26	20	
		G84	1.13	17	15	
	Parp-1$^{-/-}$	G80	1.97	39	20	26±4.2
		G83	1.86	70	38	
		G86	1.67	43	26	
		G92	1.35	27	20	

*Significant difference between *Parp-1*$^{+/+}$ and *Parp-1*$^{-/-}$ mice ($P=0.038$)

Table 2 Mutation types and their frequencies in *red/gam* genes after treatment with BHP

Mutation type	Parp-1$^{+/+}$		Parp-1$^{-/-}$		*Fold-increase by* Parp-1 *deficiency*	
	No. of mutants (%)	*Specific mutation frequency±s.e. ($\times 10^{-6}$)*	*No. of mutants (%)*	*Specific mutation frequency±s.e. ($\times 10^{-6}$)*	*Fold*	P-*value*
Deletion	69 (85)	13.1±2.1	154 (88)	22.1±4.2	1.7	0.082
1 bp	34 (42)	6.4±1.7	75 (43)	10.5±2.4	1.7	0.15
2 bp–1 kbp	19 (23)	3.7±0.96	33 (19)	5.0±1.2	1.3	0.47
>1 kbp	16 (20)	3.0±0.44	46 (26)	6.6±1.3	2.2*	0.021
Base substitution	11 (14)	2.1±0.23	12 (7)	1.7±0.31	0.81	0.31
1–2 bp insertion	1 (1)	0.17±0.17	9 (5)	1.3±0.47	7.9	0.091
Total	81 (100)[a]		175 (100)[b,a]			

*Significant difference in the frequency of >1 kbp deletion mutations between *Parp-1*$^{+/+}$ and *Parp-1*$^{-/-}$ mice ($P<0.05$). [a]Identical mutants derived from the same mouse were counted as one mutation. [b]One Spi⁻ mutant from *Parp-1*$^{-/-}$ mice did not contain any mutation in *red/gam* genes and was excluded from the table

difference was not statistically significant ($P=0.082$). The Spi⁻ mutants were classified into three classes based on the deletion sizes, namely deletions of single base, 2 bp–1 kbp, and >1 kbp, and we calculated each specific mutation frequency. The mutation frequencies of deletions larger than 1 kbp in *Parp-1*$^{-/-}$ mice were 2.2-fold higher than in *Parp-1*$^{+/+}$ mice ($P<0.05$). We also noticed that the specific mutation frequencies of 1–2 bp insertions in the *red/gam* genes were also 7.9-fold more in *Parp-1*$^{-/-}$ than in *Parp-1*$^{+/+}$ mice (Table 2), although the difference was not statistically significant ($P=0.091$). Notably, most of these insertions (8/9) were observed in mononucleotide adenine (thymine) runs in *Parp-1*$^{-/-}$ mice (Table 3). These 1 bp insertion and base substitution mutations might not be detected as Spi⁻ mutants if other P2 lysogenic *Escherichia coli* strain, such as WL95 (P2), were used (Nohmi and Masumura, 2004). In all, 71 and 80% of the single base deletions were located at 2–6 bp runs in *Parp-1*$^{+/+}$ and *Parp-1*$^{-/-}$ mice, respectively, and the sites of single base deletions in the *gam* gene of *Parp-1*$^{-/-}$ mice exhibited a wider distribution pattern, as shown in Figure 2. The locations of the hot spots for the single base deletions were neither different between genotypes nor from those reported for spontaneous mutations in the liver (Masumura *et al*., 2002).

Classification of BHP-induced deletion mutations with two bases or more

There was no difference in the distribution pattern of deletion mutations with two bases or more between the genotypes (Figure 3). Deletions of two bases or more were further categorized into simple- or complex-type deletions, including deletions with small insertions of 1–5 bp, recombinations, and rearrangements, by analysis of their deletion region/junction sequences (Table 4). Although the majority of the deletions were simple deletions both in *Parp-1*$^{+/+}$ and *Parp-1*$^{-/-}$ mice, the

Table 3 Insertion mutation of single or two bases in the *red/gam* genes of BHP-treated mice

	Mutant identification no.	*Insertion mutation*	*Original sequence (5′–3′)*	*Mutated sequence (5′–3′)*	*Insertion position in the* gam *gene*
Parp-1$^{+/+}$	Ls4 G81-1-8	c	gct*c*aga	gct*cc*aga	157
Parp-1$^{-/-}$	Ls6 G92-1-2	t	gtc*tt*gag	gtc*ttt*gag	149–150
	Ls6 G92-2-5	a	agc*aaaaaaa*tcc	agc*aaaaaaaa*tcc	295–300
	Ls13 G92-1-4	a	agc*aaaaaaa*tcc	agc*aaaaaaaa*tcc	295–300
	Ls4 G83-2-8	aa	agc*aaaaaaa*tcc	agc*aaaaaaaaa*tcc	295–300
	Ls13 G83-1-3	c	tggcaga	tgg*cc*aga	350
	Ls4 G80-1-10	a	ttg*aaa*cca	ttg*aaaa*cca	374–376
	Ls4 G80-2-9	a	ttg*aaa*cca	ttg*aaaa*cca	374–376
	Ls4 G80-2-13	a	ttg*aaa*cca	ttg*aaaa*cca	374–376
	Ls4 G83-1-10	a	ctc*a*cca	ctc*aa*cca	386

Underlined italic letters represent the sites of mutations

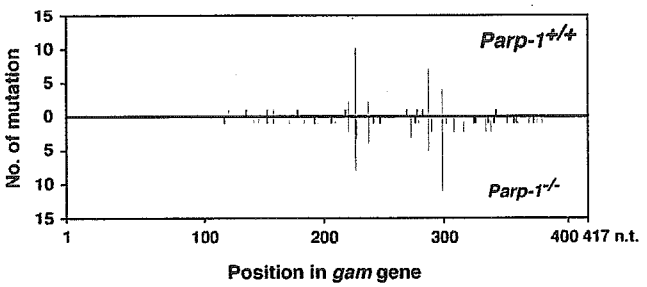

Figure 2 Distribution of single-base deletion mutations in the *gam* gene. Red bars indicate single-base deletions in a run of two to six bases of the same nucleotide; black bars indicate those not located in identical run sequences. Nucleotide 1 corresponds to the adenine residue in the first ATG of the *gam* gene. Total single base deletions show a wider distribution pattern in *Parp-1*$^{-/-}$ than in *Parp-1*$^{+/+}$ mice

ratio of complex-type deletions was significantly higher in *Parp-1*$^{-/-}$ compared to *Parp-1*$^{+/+}$ mice ($P<0.05$).

Mutants accompanying small insertions at the junction of deletions were observed in six of 73 (8.2%) in *Parp-1*$^{-/-}$ but none in *Parp-1*$^{+/+}$ mice (Table 4). Deletion mutants could be categorized into two types depending on the structures of the deletion junctions. If they harbor microhomology, they could possibly be produced during microhomology-mediated end joining (MEJ) and be classified as MEJ type (Figure 4) (Roth and Wilson, 1986). If the deletion junctions harbor no microhomology, they could possibly originate during non-microhomology-mediated end joining (non-MEJ) and could be classified as non-MEJ type (Figure 4). In non-MEJ, DNA termini are postulated to be processed to become blunt ended, and then both ends will be held together and ligation of DNA ends will be accomplished (Roth and Wilson, 1986).

Notably, five out of the six mutants from *Parp-1*$^{-/-}$ mice harbored no microhomology at deletion junctions, indicating that they were mostly caused by non-MEJ. Three mutants contained palindromic small insertions at deletion junctions (see the legend of Table 4).

Seven mutants from *Parp-1*$^{-/-}$ and two from *Parp-1*$^{+/+}$ mice (Table 4) were found to contain rearrangements (see Materials and methods for experiments). We also noticed that three mutants from *Parp-1*$^{-/-}$ mice accompanied recombinations, which occurred between the deleted regions of the *red/gam* genes and sequences in lambda EG10 (Table 5). As the lambda EG10 sequence is tandemly integrated in the genome, we could not determine whether these complex-type deletions were generated by reciprocal or nonreciprocal recombinations. Interestingly, two out of the three mutants harbored microhomology at the deletion junctions. On the other hand, the deletion in Ls4 G86-2-6 (Table 5) was suggested to occur through two sequential recombinations using 8–10 bp homologous sequences (underlined sequences in Table 5). Notably, 'Cttca' at junctional sequences of the deletion was common in two out of the three rearrangements (Table 5).

The fraction of deletion mutants that harbored short microhomology at the deletion junction, namely MEJ type to the total NHEJ event (the sum of MEJ-type and non-MEJ-type deletions), was 13/30 (43%) and 17/66 (26%) in *Parp-1*$^{+/+}$ and *Parp-1*$^{-/-}$ mice, respectively, showing a tendency for decrease of MEJ-type and increase of non-MEJ-type under *Parp-1* deficiency, although the difference is not statistically significant ($P=0.085$).

Discussion

The Spi$^-$ mutant frequencies were 1.6-fold higher in the liver of *Parp-1*$^{-/-}$ compared to *Parp-1*$^{+/+}$ mice after the treatment with BHP ($P<0.05$). Most of the mutations were found to be deletion types in both genotypes, and the specific mutation frequencies of deletion showed a 1.7-fold elevation in *Parp-1*$^{-/-}$ compared to *Parp-1*$^{+/+}$ cases, although the difference was not statistically significant ($P=0.082$). We further observed that *Parp-1* deficiency enhances deletion mutations, especially more than 1 kbp in size ($P<0.05$), and complex-type deletions accompanying either insertion or recombination/rearrangement in mice after treatment with BHP ($P<0.05$). On the other hand, the mutant frequencies in the *gpt* gene were elevated to the same level in both *Parp-1*$^{+/+}$ and *Parp-1*$^{-/-}$ mice, suggesting that *Parp-1*

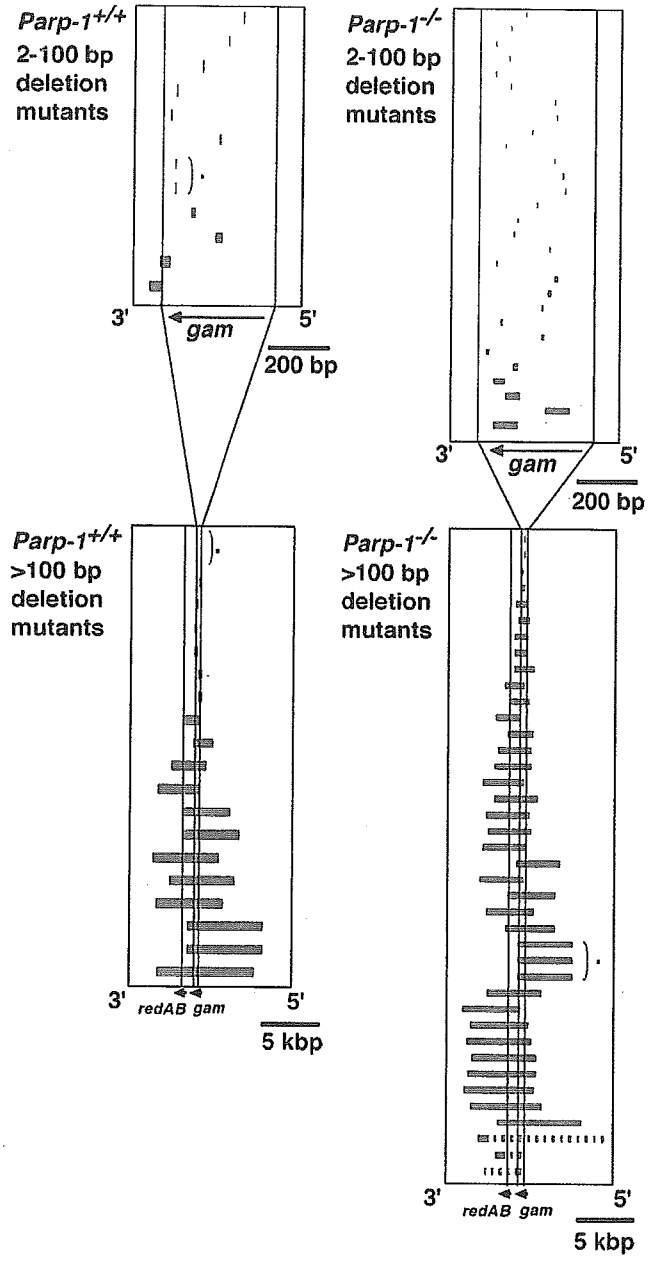

Figure 3 Distribution pattern of deletion mutations in the *red/gam* genes of the indicator bacteriophage. The two upper panels (**a**, **b**) show deletion of 2–100 bp. The two lower panels (**c**, **d**) show deletion of greater than 100 bp. The two left-hand panels (**a**, **c**) show the results in *Parp-1*$^{+/+}$, and the two right-hand panels (**b**, **d**) show the results in *Parp-1*$^{-/-}$ animals. Each red horizontal bar represents all observed deletions. The length of the bar indicates the size of the deletions. The horizontal axis shows the lengths of the genes that were used. The position of the bar shows the regions deleted in each example. The vertical axis has no significance. The individual observations are simply listed in measuring the sizes of the deletions. *Identical mutants from the same mouse

deficiency does not contribute substantially to the increase of point mutations even after treatment with the alkylating agent. The data suggested that *Parp-1* deficiency led to the enhancement of deletion mutation frequency after treatment with an alkylating agent, BHP, and this may directly relate to the higher incidence

Table 4 Classification of deletion mutations of two bases or more in the *red/gam* genes in BHP-treated mice

Deletion	No. of mutants					
	Parp-1$^{+/+}$			Parp-1$^{-/-}$		
	Total	*MEJ*	*Non-MEJ*	*Total*	*MEJ*	*Non-MEJ*
Simple	30	13	17	57	16	41
Complex-type						
With small insertion	0	0	0	6 *	1	5[a]
With recombination	0	0	0	3	0	3
With rearrangement	2	ND	ND	7	ND	ND
Total	32			73		

*Significant difference in complex-type deletion between *Parp-1*$^{+/+}$ and *Parp-1*$^{-/-}$ mice ($P = 0.047$). MEJ, microhomology-mediated end joining. Non-MEJ, nonmicrohomology-mediated end joining. ND, not determined. [a]Three mutants contained palindromic small insertions at deletion junction: 5′-GCCTCTTTCTCTTCA*a*TGCTGGTAGT-GACGC-3′, 5′-GCTCATGTAATTTAT*ta*TAGTGAATGCTTTTG-3′, and 5′-CGGGCGAGCTGCTGG*cc*CGCGCCCAGCTCTGAGC-3′. Lowercase and underlined sequences indicate small insertions and palindromic sequences, respectively

of cancer development. Spontaneous mutant frequencies in bone marrow cells measured by both *gpt* and Spi$^-$ assays were not different between *Parp-1*$^{+/+}$ and *Parp-1*$^{-/-}$ animals at 4 months old ($P > 0.05$, respectively). This was expected since spontaneous tumor incidences, including those of lymphoma, were not elevated in *Parp-1*$^{-/-}$ mice at least until 9 months of age (Nozaki *et al.*, 2003), and the elevation of the incidence of hepatocellular carcinoma in *Parp-1*$^{-/-}$ mice was reported only at 18–24 months (Tong *et al.*, 2002). To understand the relationship of mutation and carcinogenesis, it will be helpful to measure mutant frequencies in *Parp-1*$^{+/+}$ and *Parp-1*$^{-/-}$ mice at advanced ages.

BHP mainly produces O^6- and N^7-methylguanines, and O^6- and N^7-hydroxypropylguanines as DNA lesions (Kokkinakis, 1992). O^6- and N^7-methylguanines can be repaired by BER or alkylguanine alkyltransferases, whereas O^6- and N^7-hydroxypropylguanines might be repaired not only by BER but also by nucleotide excision repair (Nivard *et al.*, 2003). Point mutations in the *gpt* gene after treatment with BHP are likely to be caused by translesion DNA synthesis through damaged bases. It was notable that the frequencies of 1–2 base adenine (thymine) insertions in the adenine (thymine) mononucleotide run sequences in *red/gam* genes showed a greater tendency in *Parp-1*$^{-/-}$ than in *Parp-1*$^{+/+}$ mice, although it was not statistically significant. These mutations could be caused by DNA polymerase slippage during replication. There is a possibility that either the frequencies of DNA polymerase slippage are higher or the subsequent mismatch repair is less efficient under *Parp-1* deficiency.

In the BER process, damaged bases are initially excised by DNA glycosylases, such as 8-oxoguanine-DNA glycosylase (OGG1) or endonuclease III homolog 1 (NTH1), and, subsequently, a single base gap is

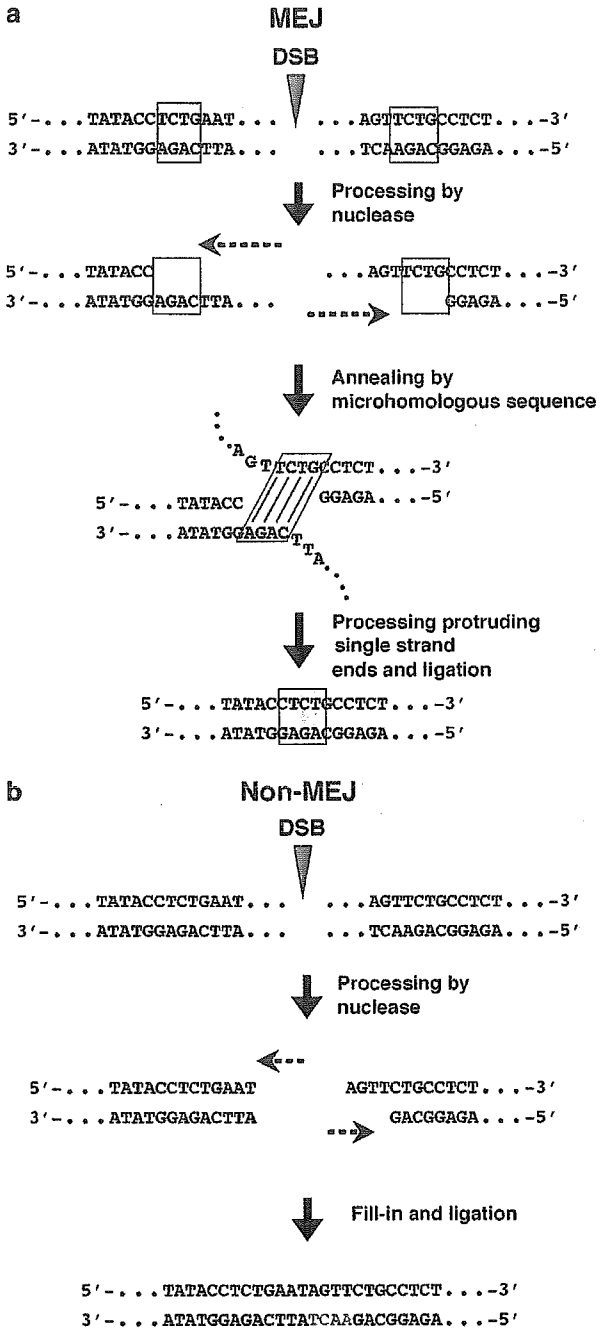

Figure 4 MEJ and non-MEJ reactions after introduction of DSB. (**a**) MEJ: After occurrence of DSB, both of the DNA termini are processed by nucleases, for example, Artemis, Mre11 or Werner syndrome protein (Paull and Gellert, 2000; Oshima *et al*., 2002; Lieber *et al*., 2003). When both ends reach a microhomologous sequence of 2–5 bases, excision of DNA is stopped and annealing occurs. After removing protruding single-stranded ends, ligation of both the strands occurs and the end-joining process is completed (Roth and Wilson, 1986). (**b**) Non-MEJ: Both DNA termini are either blunt ended when DSB occurred or processed to become blunt ended by nucleases. Then, both DNA ends may be held together by DNA-PKcs, Ku70/80, XRCC4 complex, and ligation of DNA ends will be carried out, probably by DNA ligase IV (Roth and Wilson, 1986)

generated by AP endonuclease activity, and nick sensor Parp-1 is recruited to DNA ends (Menissier-de Murcia *et al*., 1989). At later stages in BER, especially in the long-patch repair, Parp-1 facilitates DNA polymerization by interacting with polβ (Dantzer *et al*., 2000). Parp-1 also interacts with FEN-1, which excises approximately 2–7 base pairs to remove damaged bases in the long-patch repair (Prasad *et al*., 2001). The absence of difference in the mutant frequency of the *gpt* gene between *Parp-1*$^{-/-}$ and *Parp-1*$^{+/+}$ mice ($P>0.05$, see Supplementary Information) suggested that the BER pathway under *Parp-1* deficiency might possibly proceed until the excision of damaged bases.

The increase of deletion mutations accompanying insertion or recombination/rearrangement ($P<0.05$, see Table 4) indicated two possibilities, namely, DSB repair occurred more frequently or the repair fidelity of DSBs was lower under *Parp-1* deficiency. As for the former possibility, a possible explanation is that DNA polymerization or the displacement step of BER might be stalled in the absence of Parp-1 by the inefficient recruitment of repair proteins and DNA gaps may not be sealed efficiently and properly. The experiment with the *in vitro* reconstituted system showed that Parp-1 stimulates strand displacement and the removal process of long patch repair in the presence of FEN-1 (Prasad *et al*., 2001). It is generally postulated that the stalled, gapped DNA intermediates in BER could possibly develop into DSBs (Harrison *et al*., 1999; Vispe *et al*., 2003). The DSBs might also be induced at a higher frequency in the absence of Parp-1 after treatment of BHP by stalled replication forks caused by the damaged bases, leading to a collapse of the holiday structure. It is shown that, in *Parp-1*$^{-/-}$ cells, the repair of stalled replication forks is delayed (Yang *et al*., 2004). Another possibility for generation of DSB after BHP treatment is that, in order to remove massive alkylated bases, abortive mismatch repair (Branch *et al*., 1993) or base excision repair (Blaisdell and Wallace, 2001) might occur and excessive incision reactions on DNA may result in introduction of DSBs.

The second possibility, namely lower fidelity of DSB repair under *Parp-1* deficiency, could be explained as follows. DSBs could be repaired mostly by either NHEJ or HR (Valerie and Povirk, 2003), and, because we found no long homology in the junctional sequences of any of the analysed simple deletion mutants, we suggest that most of the deletion mutations might be generated during NHEJ repair. The major process of NHEJ is catalysed by DNA-PKcs and the Ku70/80 complex. In the presence of both DNA-PKcs and Parp-1, autophosphorylation of DNA-PKcs is stimulated by Parp-1 (Ariumi *et al*., 1999). Parp-1 might also protect DSB termini from nuclease attack because polyADP-ribosylation of Ku70/80 reduces exonuclease activity of WRN *in vitro* (Li *et al*., 2004) and contributes to efficient recruitment and activation of DNA–PK complexes. It is thus speculated that the recruitment of DNA-PKcs or its activity could not be controlled in the absence of Parp-1, resulting in low fidelity of NHEJ repair.

Table 5 Complex-type deletion mutations accompanying recombination observed in *Parp-1*$^{-/-}$ mice

Mutant identification no.	*Original sequences (I) in lambda EG10*	*Original sequences (II) in lambda EG10*	*Junctional sequence of mutation*
Ls4 G80-1-2	5′-…CGCCCGTTTTctggatgcgg-3′ 3′-…GCGGGCAAAAgacctacgcc-5′ * * 13754[a] 13763	↓ 5′-…GGTGATGTCTtcaagtggag-3′ 3′-…CCACTACAGAagttcacctc-5′ * * 20625 20634	5′-…GGTGATGTCTAAAACGGGCG…-3′ 3′-…CCACTACAGATTTTGCCCGC…-5′
Ls4 G86-2-6	5′-cccggtggtctgCCCTGG…GGCTGCaggtgcagagtgat-3′ 3′-gggccaccagacGGGACC…CCGACGtccacgtctcacta-5′ * * 14354 14381 5′-…GCGTGGTCTGagtgtgttac-3′ 3′-…CGCACCAGACtcacacaatg-5′ * * 18893 18902	↓ 5′-…CCTGCTCTGCCGCTtcacgcagtg-3′ 3′-…GGACGAGACGGCGAagtgcgtcac-5′ * * 22456 22465	5′-…CTCTGCCGCTGCAGCC…CCAGGGCAGACCACGC…-3′ 3′-…GAGACGGCGACGTCGG…GGTCCCGTCTGGTGCG…-5′
Ls13 G83-1-6	5′-…ATTATGGGCCgccacgacga-3′ 3′-…TAATACCCGGcggtgctgct-5′ * * 1992 2001	↓ 5′-gggtatcatgTAGCCGCTTA…-3′ 3′-cccatagtacATCGGCGAAT…-5′ * * 26359 26368	5′-…ATTATGGGCCTAGCCGCTTA…-3′ 3′-…TAATACCCGGATCGGCGAAT…-5′

Lowercase indicates deleted sequences, and homologous sequences at junctions are underlined. Red and blue letters represent rearranged sequences. The *red/gam* gene is located at nucleotide positions from 24 921 to 23 450 in the sense orientation. [a]Nucleotide positions (as indicated by asterisk) in lambda EG10. ↓, the position of the deletion junctions. The upper red line indicates 'Cttca' sequences at deletion junctions, which is common to Ls4 G80-1-2 and Ls4 G86-2-6.

NHEJ is further classified into MEJ and non-MEJ; the former harbors some microhomology at DSB termini, whereas the latter harbors no microhomology (Figure 4). To ask whether the deletion mutations observed in *Parp-1*$^{-/-}$ and *Parp-1*$^{+/+}$ mice were caused through MEJ or non-MEJ, we categorized the Spi$^-$ mutants and calculated the fraction of MEJ frequency to total NHEJ events. The fraction is decreased to approximately half that in *Parp-1*$^{-/-}$ (26%) compared with that in *Parp-1*$^{+/+}$ mice (43%). We also found that the frequency of complex-type deletions accompanying 1–5 bp insertions or recombination/rearrangement is substantially increased ($P<0.05$), namely, 16/73 (22%) of the mutants in *Parp-1*$^{-/-}$ compared to 2/32 (6%) of those in *Parp-1*$^{+/+}$ cases (Table 4). In most of these cases, the deletion junction did not harbor microhomology. These results suggest that DNA ends may be destabilized in the absence of Parp-1 and allow accidental insertion or recombination/rearrangement in non-MEJ processes. The introduction of small insertions in deletion junctions could be caused by polymerase λ (pol λ) and pol μ, which facilitate filling of a few bases gap in the NHEJ, and terminal deoxynucleotidyl transferase (TdT), which is also involved in the NHEJ event of V(D)J recombination (Garcia-Diaz *et al.*, 2002; Bebenek *et al.*, 2003). In the absence of Parp-1, these error-prone DNA polymerases might easily modify these DNA ends, resulting in small insertions, namely nontemplated nucleotides.

Three of six mutants with small insertions contained 'palindromic (P) nucleotides' at deletion junctions under *Parp-1* deficiency (Table 4). 'P nucleotides' are possibly introduced by self-complementary single-strand extensions during the DSB repair process of V(D)J recombination, and slightly longer 'P nucleotides' insertions at a higher frequency could be observed in the deletion mutations of SCID mice (Ding *et al.*, 2003). The present results suggested the possibility that 'P nucleotides' may be preferentially introduced during NHEJ repair under *Parp-1* deficiency, possibly through the destabilization of DNA ends.

A higher frequency (10/73) of deletion mutations accompanying recombination/rearrangement was observed in *Parp-1*$^{-/-}$ animals than in *Parp-1*$^{+/+}$ animals (2/32) as shown in Table 4, although it is not statistically significant ($P>0.05$). Ls4 G86-2-6 mutation in Table 5 was suggested to involve two sequential recombinations using 8–10 bp homology (underlined). There is a possibility that this mutation could be caused by the switchover of NHEJ to HR repair during processing of DSBs. The possible involvement of Parp-1 in the regulation of switching from NHEJ to HR should be further investigated, because the elevated frequency of HR including gene targeting (Semionov *et al.*, 2003) and SCEs (de Murcia *et al.*, 1997) was reported previously in the absence of Parp-1 or by Parp-1 inhibition.

We observed more deletion mutations ($P=0.082$), especially those more than 1 kbp ($P<0.05$), and complex-type deletions accompanying either insertion or recombination/rearrangement ($P<0.05$) in *Parp-1*$^{-/-}$ mice. We suggested that this indicates that Parp-1 prevents these types of genomic changes. *In vitro* studies showed that Parp-2 also facilitates BER by interacting with DNA repair proteins such as XRCC1 (Schreiber *et al.*, 2002); however, the present result suggests that the role of Parp-1 in preventing these types of mutations could not be fully compensated by Parp-2 or other molecules engaged in DNA repair. It is reported that interstitial deletions in human cancer could be preferentially produced through NHEJ repair processes (Sasaki *et al.*, 2003), suggesting the substantial contribution of deletion mutation to carcinogenesis. Although the increase of Spi$^-$ mutant frequency by *Parp-1* deficiency is only 1.6-fold ($P<0.05$), this difference may evoke a significant impact on multi-step carcinogenesis (Doll, 1962; Sugimura, 1992). For example, if mutation in five genes is necessary for cancer development, the difference in the frequency of achieving all the five mutations between *Parp-1*$^{+/+}$ and *Parp-1*$^{-/-}$ mice is calculated to be 10-fold. The impact of *Parp-1* deficiency on deletion mutation might be different among tissues and DNA-damaging insults; however, the present results suggest a substantial role of Parp-1 in the maintenance of genomic stability, which may be important not only for carcinogenesis but also for various pathogenic processes. The results also raise a caution on the therapeutic use of Parp-1 inhibitors, and basic studies should be carried out carefully to avoid any possible risks to causing somatic or germ-cell mutations by Parp-1 inhibition.

Materials and methods

Establishment of Parp-1$^{-/-}$/gpt *delta mice*

Homozygous *gpt* delta transgenic mice of C57BL/6 genetic background (Nohmi *et al.*, 1996) were mated with *Parp-1*$^{-/-}$ mice of ICR/129Sv mixed genetic background (Masutani *et al.*, 1999), and *Parp-1*$^{+/-}$ mice homozygous for the lambda EG10 transgene (*Parp-1*$^{+/-}$*/gpt* delta mice) were obtained. By intercrossing *Parp-1*$^{+/-}$*/gpt* delta mice, we obtained *Parp-1*$^{-/-}$*/gpt* delta and *Parp-1*$^{+/+}$*/gpt* delta animals.

Animal treatment

Spontaneous mutant frequencies in the bone marrow and livers were analysed as follows. Male *Parp-1*$^{+/+}$ and *Parp-1*$^{-/-}$ mice ($n=5$, respectively) were fed a basal diet (CE-2, Clea Japan), anesthetized, and killed at the age of 16 weeks. The bone marrows and livers were immediately frozen in liquid nitrogen, and stored at −80°C until DNA extraction.

BHP (Nakalai Tesque) was dissolved in saline, adjusted to 0.2 g/ml, and sterilized by filtration. Four *Parp-1*$^{-/-}$*/gpt* delta and four *Parp-1*$^{+/+}$*/gpt* delta male mice received an intraperitoneal injection of BHP at 2 g/kg body weight (bw) at the age of 16 weeks. All animals were killed 1 week after BHP administration, and the livers were frozen and stored as described above. Genomic DNAs were extracted from the bone marrows and livers by standard phenol/chloroform extraction or the dialysis method performed with a Recover-Ease DNA isolation kit (Stratagene). A lambda phage *in vitro* packaging reaction was carried out with Transpack Packaging Extract (Stratagene). The experimental protocol was approved